Chemical Events in the Atmosphere and their Impact on Environment
Pontifical Academy of Sciences, *Scripta Varia* 56, Vatican City 1985
www.pas.va/content/dam/accademia/pdf/sv56/sv56-canuto.pdf

THE YOUNG SUN, THE EARLY EARTH AND THE PHOTOCHEMISTRY OF OXYGEN, OZONE AND FORMALDEHYDE IN THE EARLY ATMOSPHERE

V.M. CANUTO*†, J.S. LEVINE**, C.L. IMHOFF+, I. GOLDMAN*,
T.R. AUGUSTSSON**, and O. HUBICKYJ*

1. The Primitive Nebula

While cosmogony, i.e. the study of the origin of the solar system, has interested scientists for centuries, it is only in the seventeenth century that the first well posed model of the origin of the solar system was proposed. In 1644, R. Descartes proposed the "vortex theory" whereby the entire universe was made up of vortices which eventually ended up as planets. It must be noted that the idea of vortices evokes turbulence which, as we shall see, plays a basic role in the evolution of the solar nebula. In 1745, Buffon suggested that the solar system was formed out of the material torn away from the sun by a passing object. Having no way of calculating the probability of stellar encounters, there was no way to confirm or refute Buffon's suggestion. (Buffon's hypothesis must have certainly pleased those who believed in the uniqueness of our solar system, since a close encounter of two stars, or a star and a comet as Buffon suggested, must have been considered an infrequent event). Today we know that the probability for two stars to encounter during the entire age of the Universe is so small as to make Buffon's model unacceptable.

Ten years later, in 1755, I. Kant proposed a rather modern theory, that of a rotating gas cloud that flattened into a disc which then somehow

* NASA, Goddard Institute for Space Studies, New York, N.Y. 10025
† Also with Dept. of Physics, CCNY, N.Y.
** NASA, Langley Research Center, Hampton, Va 23665
+ Computer Sciences Corporation, Astronomy Dept., Silver Spring, Md. 20910

broke into separate rings or planets. In 1796, P.S. Laplace first spoke of a "Solar Nebula, SN", a term now commonly used when referring to the origin of the solar system. One serious problem however remained: if things occurred this way, the sun should still be rotating at a near rotational breakup, i.e. its period should be

$$P = 0.02 \text{ days} \tag{1}$$

while the observed value is

$$P = 25.3 \text{ days} \tag{2}$$

How did the sun get rid of its spin angular momentum? The discovery of acceptable mechanisms for the transfer of angular momentum has been one of the major reasons why the Nebular Hypothesis has gained general acceptance. First is the realization that the sun is continually losing matter through a strong wind which, near the sun, is forced to flow along the magnetic field lines determined by the sun's magnetic field. This generates a strong magnetic torque that can remove angular momentum from the sun (Mestel, 1968 a,b). How efficiently this angular momentum can subsequently be redistributed to the entire nebula depends on physical processes linked to turbulence. Before reviewing recent work on the evolution of the solar nebula and the subsequent formation of planets, we shall discuss the stages of star formation believed to lead to a protosun and an accompanying solar nebula.

2. A Fragmentation Process. A Difficulty

There is convincing observational evidence that the placental interstellar medium (ISM) from which the solar system originated was a dense molecular cloud (Wasserburg *et al.*, 1982; 1979). In fact, the recent evidence of the presence of short-lived nuclei in meteorites requires that the free-fall time scale for gravitational collapse (t_{ff}) be less than or comparable to the mean lifetime of ^{26}Al ($\sim 10^6$ yrs), i.e. $t_{ff} \leqslant 4.10^7/\sqrt{n_H} < 10^6$ yrs, which requires $n_H \gtrsim 10^3$/cc, a value typical of molecular clouds. Since molecular clouds are observed to be a major feature in our galaxy, they constitute a most reliable starting point for the processes that will eventually lead to the formation of stars and planetary systems (Falk and

Schramm, 1979). A detailed analysis of the events that take place in such clouds, after an external agent has caused them to become unstable, has been worked out for a large variety of initial conditions (Bodenheimer, 1978; 1981). Typically: $M/M_\odot = 10^4$, $\rho = 1.7\ 10^{-23}$ g/cc, $T = 75°K$, $R = 6.6\ 10^{19}$ cm, $\Omega = 10^{-15}$ rad/sec, and $J/M = 1.75\ 10^{24}$ cm^2 sec^{-1}. Since T-Tauri stars have $J/M = (10^{17} - 10^{18})$ cm^2 sec^{-1}, a major effort has been dedicated to understand how to achieve a reduction of about 6 orders of magnitude in the value of J/M. The analysis indicates that the J/M reduction may be best achieved via a hierarchy of collapse and fragmentation and that the process yields binary fragments, a reassuring result in view of the preponderance of binary star systems. The most relevant result of these computations is that the fragments form with masses *larger* than the local Jean masses, ensuring their continuous collapse, thus placing, the hierarchical fragmentation model on firm foundations (Boss, 1982). Recent work by Boss (1983) has however indicated difficulties with the previous scenario. Study of the collapse of a dark cloud ($M = 50\ M_\odot$, $T = 10°K$, $R = 2 \times 10^{18}$ cm, $\Omega = 3 \times 10^{-14}$ rad sec^{-1}, $J/M = 4.10^{22}$ cm^2 sec^{-1}) indicates that a binary system is first formed with $M/M_\odot = 8$, each of the two fragments dividing further into a triple system with $M/M_\odot = 2$, $R = 2.10^{15}$ cm, $J/M = 10^{20}$ cm^2 sec^{-1}. The dynamics of each triple system indicates (Agekyan and Anosova, 1968) that one object will be ejected in a time scale of $t \approx 10^5$ yrs, thus isolating one of the three partners. A recent study by Boss (1983) of the fate of the 2 $M_\odot$ ejected body indicates that it will further fragment into a multiple system, a process that will stop only at $M < .1\ M_\odot$. These results show that fragmentation is not a self-regulating mechanism until $M \sim 10^{-2}\ M_\odot$, in agreement with a result by Low and Lynden-Bell (1976) on opacity limited fragmentation. Boss's analysis casts serious doubts on whether the solar system actually originated through an inviscid fragmentation process. The difficulty remains unresolved.

3. Mass and Evolution of the Solar Nebula. The New Convective Model

If one assumes that the solar nebula had a solar composition, then one can obtain a *lower limit* for its mass M_N. Following Hoyle's procedure (1962), we have

Constituents	Jupiter Saturn H, He (~1)	Uranus Neptune C,N,O (1.5%)	Terrestrial Planets Mg, Si, Fe (0.25%)
Present Mass ($10^{-5}\,M_\odot$)	124	9.6	.6
Multiplier	1	67	400
Augmented Mass ($10^{-5}\,M_\odot$)	124	643	240

The result is therefore that the mass of the nebula M_N must have been larger than

$$M_N > 10^{-2}\,M_\odot \text{ or } M_N > 7.5\,M_{NO} \tag{3}$$

where $M_{NO} = 1.34\ 10^{-3}\,M_\odot = 448\,M_\oplus$ is the present mass.

Since the sun is located at the center of such nebula, one may expect that the nebular temperature T vs. R, the radial distance from the sun, would be determined roughly by

$$\frac{L}{4\pi R^2} \simeq \sigma T^4 \tag{4}$$

i.e. that

$$T \sim R^{-1/2} \tag{5}$$

This is however not the case. Through careful analysis of the temperature required for the condensation of various chemical elements, Lewis (1972, 1974) has derived the relation

$$T \sim R^{-1}, \tag{6}$$

leading one to conclude that the primary source of thermal energy in the nebula could not have been solar energy alone. Today it is generally believed that the primary source of energy was the release of gravitational energy of material that fell toward the protosun.

Consider in fact a disc in which the fluid elements follow Keplerian orbits, i.e., the fluid is in a state of differential rotation $\Omega = \Omega(R)$. This implies a non-zero rate of shearing $R\,d\Omega/dR$.

If there is *viscosity* present, its effect would be that of damping out the shearing motion, whose energy content will be dissipated into heat to

be then radiated away (Pringle, 1981). Thus, viscosity causes the fluid to lose energy. Since the only available energy is the gravitational binding energy, the material will spiral inward to lower energy and angular momentum levels. As a result, mass is transferred inward and angular momentum is transferred outward.

The equations governing the disc are given by Pringle (1981) as ($v_\Phi = \Omega R$)

$$R \frac{\partial \Sigma}{\partial t} + \frac{\partial}{\partial R}(R \Sigma v_R) = 0 ,$$

$$R \frac{\partial}{\partial t}(\Sigma R^2 \Omega) + \frac{\partial}{\partial R}(\Sigma R^3 \Omega v_R) = \left(\frac{\partial}{\partial R} \right) \bar{\nu} \Sigma R^3 \frac{\partial \Omega}{\partial R} \tag{7}$$

representing conservation of mass and angular momentum respectively. Σ is the surface density at R, $\bar{\nu}$ is an average effective viscosity at R, Ω is the angular velocity and v_R is the radial velocity.

For the case of a Keplerian steady disc, eqs. (7) can be integrated and combined to yield

$$- 2 \pi R \Sigma v_R = 3 \pi \bar{\nu} \Sigma = \dot{M} \tag{8}$$

where the constant of integration $\dot{M}$ has the physical interpretation of a rate of mass accretion toward the central object.

The heat generated by viscosity must be transported away from the midplane to the surface layer of the nebula, in order for the nebula to attain thermal equilibrium. It follows that at any given distance R from the central sun, there must exist a flux F that carries away such heat, i.e. we must have

$$\frac{1}{\rho} \frac{dF}{dz} = \frac{9}{4} \bar{\nu} \frac{GM}{R^3} , \tag{9}$$

where in general

$$F = F_r + F_c$$

Here F_r is the radiative flux and F_c the convective flux,

$$F_r = \frac{4acT^3}{3k_{op}\rho}\left(-\frac{\partial T}{\partial z}\right) \equiv c_p\ \rho\ \chi_r\left(-\frac{\partial T}{\partial z}\right) \tag{10}$$

$$F_c = c_p\,\rho\,\chi_c\left[-\frac{\partial T}{\partial z} + \left(\frac{\partial T}{\partial z}\right)_{ad}\right] \equiv c_p\,\rho\,\chi_c\,\beta \tag{11}$$

where k_{op} is the opacity of the material in the nebula, c_p is the specific heat, and χ is the thermometric conductivity.

To complete the determination of the z-structure of the nebula, a further equation is needed, namely

$$\frac{dp}{dz} = -\left(g\,\frac{z}{R}\right)\rho\ ,\ g = \frac{GM}{R^2} \tag{12}$$

representing hydrostatic equilibrium in the z-direction, i.e. gravitational pull toward the midplane must be compensated by a pressure gradient which supports the gas above the midplane.

This completes the list of the needed equations. If one employs a theory (like the mixing length theory of convection) to compute χ_c, as well as a model for the opacity k_{op}, then eqs. (9) and (12) determine the vertical structure of the nebula, i.e. T, ρ and F vs. z, provided appropriate boundary conditions are imposed. These are usually taken to be

$$F(z=0) = 0\ ,\ F(z=H) = \sigma T_e^4\ ,\ p(z=H) = \frac{2}{3}\,\frac{g}{k_{op}}\,\frac{H}{R} \tag{13}$$

where T_e is the nebula effective surface temperature and H is the height of the nebula. Let us now discuss k_{op} and χ_c. For k_{op} it is customary to follow De Campli and Cameron (1979), who proposed that

$$k_{op} = k\,(\text{ice}) + k\,(SiO_2) + k\,(Fe_2) \tag{14}$$

where the temperature dependence of each k is of the form

$$k = k_o\,T^2 \tag{15}$$

For F, the situation is more complex. For many years it was assumed that the major contribution to F came from F_r. However, it has been

recently pointed out by Lin and Papaloizou (1980) that in parts of the nebula "*convection*" is most likely triggered by the opacity (14), so that $F_c \neq 0$. Lin and Papaloizou (1980), Lin (1981), and Lin and Bodenheimer (1982) have adopted the Mixing Length Theory (MLT) which provides expression for $\bar{\nu}$ and χ_c. In particular (a is an undetermined constant)

$$\chi_c = a\ \Lambda^2\ (g_\circ\ \bar{\alpha}\beta)^{1/2} \tag{16}$$

where the mixing length Λ, $g_\circ$ and $\bar{\alpha}$ are given by

$$\Lambda = \text{Min}\left(z, \frac{p}{g_\circ\ \rho}\right),\ g_\circ = g\ \frac{z}{R},\ \bar{\alpha} = -\left(\frac{d\ \ell n\ \rho}{dT}\right)_p \tag{17}$$

Equations (9) and (12) have been solved numerically by Lin and Papaloizou (1980) and some of their results are presented in Figures (1) and (2). Lin (1981) has also analyzed the inner region of the nebula, $R < 10^{14}$ cm, where most of the protoplanets form. When the opacity is mainly contributed by ice-grain, Lin deduced the following results (cgs units):

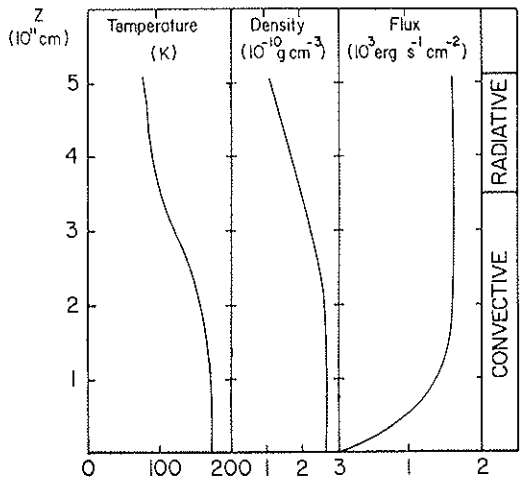

FIG. 1. The vertical structure of the nebula as from the work of Lim *et al.* (1980, 1981). Note that the convective region makes up to 2/3 of the entire z-structure. In the radiative region $\nu = 0$, and so $F =$ constant because of eq. (9). (Reproduction with permission of Dr. D.N.C. Lin).

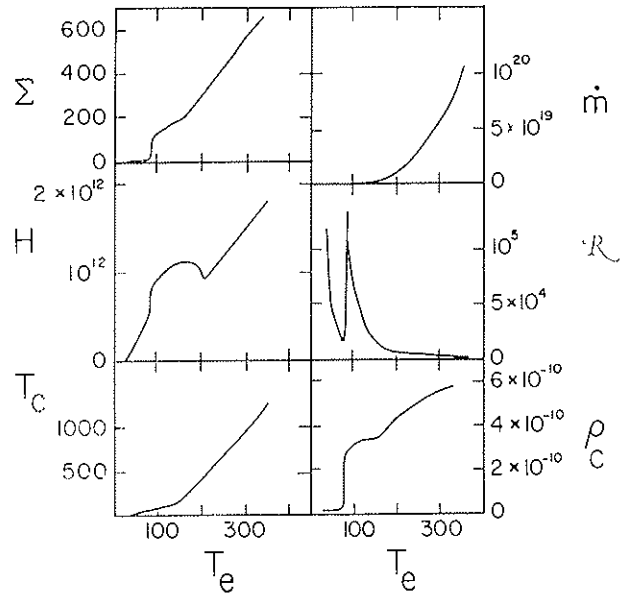

FIG. 2. Numerical solutions as a function of T_e (effective temperature) for $R = 10^{13}$ cm. The units of Σ are g cm^{-2}, those of H are cm. T_c and ρ_c are the value of T and ρ at mid-plane, $\dot{m}$ is the mass flux (g sec^{-1}). The quantity R is the Reynolds number. (Reproduction with permission of Dr. D.N.C. Lin).

$$\begin{aligned} \Sigma &= 15\ \dot{m}^{1/3}\ \alpha^{-2/3} \quad , \quad \mathrm{Re} = 7\ 10^3\ \dot{m}^{-2/3}\ r^{1/2}\ \alpha^{-2/3} \\ H &= 10^{12}\ \dot{m}^{1/3}\ r^{3/4}\ \alpha^{-1/6} \ , \quad T_c = 400\ \dot{m}^{2/3}\ r^{-3/2}\ \alpha^{-1/3} \\ \rho_c &= 2\ 10^{-11}\ r^{-3/4}\ \alpha^{-1/2} \ , \quad \tau = 300\ \dot{m}^{5/3}\ r^{-3}\ \alpha^{-4/3} \ , \end{aligned} \tag{18}$$

where $\dot{m}$ $(= \dot{M}/10^{18}$ g sec$^{-1})$ and $r = R/10^{13}$ cm; α is related to the coefficient a of eq. (16) by $\alpha = 2\sqrt{8}\ a$. (For simplicity we have assumed a molecular weight of unity, $m = 1$ and Lin's β also unity). When the opacity is determined mostly by SiO_2, like in the region near the sun, the functional forms (18) remain unchanged but the numerical coefficients vary. For example, the value 400 in T_c becomes 200.

With the knowledge of these quantities, one can evaluate the mass of the nebula M_N, as well as the time scale for its evolution. The results are

$$\begin{aligned} M_N &= 10^{28}\ (\dot{m}^{1/3}\ \alpha^{-2/3}\ r_D^2 + 5\ \dot{m}^{11/9}\ \alpha^{-10/9})\ \mathrm{g} \\ t_N &= M_N/\dot{M} = 3\ 10^2\ (\dot{m}^{-2/3}\ \alpha^{-2/3}\ r_D^2 + 6.7\ \dot{m}^{2/9}\ \alpha^{-10/9})\ \mathrm{yr} \end{aligned} \tag{19}$$

All the quantities given above depend on $\dot{m}$ and α, which cannot be evaluated a priori. In order to fix them, Lin proceeded to impose the following constraints:

(a) In order for Jupiter to be able to grow to its present mass, the Reynolds number must be less than $M_\odot/M_J$. From eq. (18), one obtains

$$\dot{m} > 1.6\ 10^3\ r_J^{3/4}\ \alpha^{-1}$$

where r_J is the initial orbital radius of Jupiter.

(b) Grains play the dual role of triggering convection and at the same time of forming the seed for planetary accretion. Since most grains condense at $1000K < T < 2000$ K, the nebular temperature must have been less than 2000K at the orbit of Mercury. This implies

$$\dot{m} < 10\ \delta_M^{9/4}\ \alpha^{1/2}$$

where $\delta_M = r_M/r_{M_0}$, r_{M_0} being the present semimajor axis of Mercury.

(c) At large distances from the protosun, the nebular material becomes transparent. Such distance must be greater than the initial orbit of Neptune r_N. From (18), one finds that the nebula remains convective if

$$\dot{m} > 30\ \delta_N^{9/5}\ \alpha^{4/5}.$$

Putting together these constraints, Lin's best fitting values for α and $\dot{m}$ were found to be

$$10 < \dot{m} < 20\ ,\ \alpha = 2$$

which implies that

$$\dot{M} = (1\text{-}2)\ 10^{19}\ \text{g sec}^{-1} = (1.5\text{-}3)\ 10^{-7}\ M_\odot/\text{yr} \qquad (20)$$

An immediate consequence of (20) is that such mass flux could not have lasted for more than a few million years, otherwise the sun would end up with a mass greater than 1 $M_\odot$. This time scale can also be compared with information derived from isotopic data. One of the most interesting discoveries in the past few years concerns the excess of Mg^{26} found in the Allende Meteorite (Lee *et al.*, 1976). This is interpreted in terms of $A\ell^{26}$ which can only be produced by a nearby supernova explosion.

What is relevant is that since its lifetime is short, $\tau \approx .5\ 10^6$ yrs, Al^{26} must have been condensed well within this time in order for it to be still present today. This period of time is consistent with the previous estimates based on eq. (20).

With the values of $\dot{m}$ and α, one can then proceed to determine other quantities of interest. For example:

1) *Mass of the solar nebula* M_N. One obtains

$$10 < M_N/M_{NO} < 20 \tag{21}$$

where M_{NO} is the present mass of the planetary system, $= 1.34\ 10^{-3}\ M_\odot = 448\ M_\oplus$. (The quantity r_0 was taken to be Neptune's distance. The upper and lower limits correspond to the case of low and high opacities respectively).

Since the value of M_N is significantly lower than required for gravitational instability to set in (Toomre, 1964; Goldreich and Lynden-Bell, 1965; Goldreich and Ward, 1973), the nebula is found to be gravitationally stable.

2) *Mass of the nebula within Jupiter's radius* M_*. One obtains

$$.6 < M_*/M_{NO} < 1.1 \tag{22}$$

Assuming that the nebula had a solar abundance ($Z = 0.015$), one finds that the total mass of heavy elements contained in the solar nebula within the distance of Jupiter is

$$M_{*Z} = (.6 - 1.1)\ M_{NO}\ Z = (4 - 7.4)\ M_\oplus \tag{23}$$

to be compared with the total mass of the terrestrial planets

$$M_{TP} = 2\ M_\oplus \tag{24}$$

The closeness of M_{*Z} and M_{TP} is considered a "dilemma" for it implies a very high efficiency in collecting the heavy elements into protoplanets. Lin therefore proposed that the formation of the terrestrial planets must have occurred prior to the formation of Jupiter when the mass of the nebula was larger and the requirements on the efficiency less stringent.

3) *Time scale for the Solar Nebula.* Using for r_D the orbital radius of Neptune, one obtains

$$t_N \cong 10^5 \text{ yrs} , \tag{25}$$

as the time available for the protoplanets to grow. By this time, most of the gas has been used up and one must conclude that the Jovian planets, being gas rich, had to be formed. For the terrestrial planets the situation is not so clear cut because all that is actually needed is that by this time a sufficient amount of heavy elements be converted into planetesimals that may at later times form planets.

The details of how they accreted the remaining mass and the corresponding time scale remain to be worked out. It seems however reasonable to expect that the end product will be a planet with a thin atmosphere since most of the gas had already been used up early on. This conclusion may be relevant to the recent suggestion by Hayashi and collaborators (1981, 1982) that the young earth may have ended up shrouded in a thick atmosphere. In Section 5, we shall discuss the work done in the field of formation of the earth and indicate that even in that case there are reasons to believe that no thick atmosphere actually formed.

The reason why we prefer to present the "standard scenario" in a separate Section is because we feel it is premature to engage in a full comparison of the two approaches since all the details are as yet not available.

One comparison however can be made. Lin's approach implies time scales *shorter* by a factor of about ten with respect to the ones discussed in Section 5. This in turn implies that the relevance of the UV radiation from the Sun may have been even greater than the one we shall discuss in Section 8.

4. *Conclusions*

While the work of Lin *et al.* is interesting in that it tries to model convective turbulence from first principles, it still contains arbitrary parameters (four) and approximations that cast doubts on the reliability of the results. Specifically, the height of the nebula H had to be chosen arbitrarily since the model as constructed by Lin *et al.* gives rise to a degenerate set of solutions for H. The arbitrariness in the choice of H

reflects on the value of the surface density (Σ), which in turn affects the value of the nebula's mass (M).

4. An Improved Model for Convective Turbulence

Having pointed out that viscosity is the key quantity for the overall behavior and structure of the nebula, we must ask ourselves what is its origin. The first possibility is evidently particle viscosity. It can however be seen that in that case, the timescale for mass redistribution would be much longer than the age of the solar system itself. Lin (1981) has also pointed out that density perturbations could not grow into protoplanets because they could not accrete material beyond their immediate vicinity.

The next phenomenon that comes to mind because of its efficiency is *turbulence*, which can be generated in a large variety of ways. Until Lin and Papaloizou's work (1980), it was generally believed that turbulence may originate from meridional currents (Mestel, 1965), infall of material onto the nebula (Cameron, 1976) and magnetic dragging of ionized nebular material (Hoyle, 1960; Hayashi, 1982). While these are physically reasonable mechanisms to boost-up the poor efficiency of particle viscosity, their actual effectiveness depends on ad hoc assumptions. Progress was achieved when Cameron (1978) suggested that turbulent *convection* is the most natural mechanism to contribute to the viscosity $\bar{\nu}$. As noted in Section 3, Lin and his collaborators (1980, 1981) adopted the Mixing Length Theory, which however cannot fix the parameter a entering in eq. (16). As discussed, Lin and his collaborators had to use other constraints to make the model fully predictable. Recently Canuto *et al.* (1984, 1985) have tried to improve on the situation by proposing a model for convective turbulence that allows α to be determined and which also offers a natural way to incorporate important physical parameters like rotation. We shall sketch here the main points of this new approach.

A complete theory of convective turbulence, if it existed, would provide an expression for the turbulent viscosity ν_t. Lacking such theory one usually writes, on dimensional grounds,

$$\nu_t = \xi \, \ell_t \, v_t \tag{26}$$

where ℓ_t and v_t are typical lengths and velocities of the turbulent medium and ξ is an unknown numerical parameter.

Following the standard description of turbulence (Landau and Lifshitz,

1959), one divides the spectrum of eddy sizes into three regions: (1) *Large* eddies $k \sim k_0$, $\ell_t \sim L$, where $L \sim k^{-1}_0$ is the size of the system itself. In the case of a disc, L is the width of the disc. This part of the spectrum contains most of the energy. (2) *Small* eddies, $k \sim k_1$, $\ell_t \sim \lambda = L/Re^{3/4}$, where Re is the Reynolds number. In region (2), energy is dissipated into heat via molecular viscosity. Finally, (3) there is the so-called inertial region, $k_0 < k < k_1$, where energy is not dissipated but simply transferred from region (1) to region (2). This region is characterized by eddies of almost all sizes, the largest ones being of the order L and the smallest ones being almost of the order λ respectively, i.e. $\lambda < \ell_t < L$. The properties of the turbulent region can be described once one knows the "energy spectrum function" E(k) (Batchelor, 1970)

$$v^2_t(k) = \int_k^\infty E(k)\, dk \,. \tag{27}$$

The determination of E(k) from first principles is the main goal of any theory of turbulence. Using dimensional arguments (Landau and Lifshitz, 1959) or a form $E(k) \sim k^{-n}$, one derives ($2r = n - 1$, $r = 1/3$ corresponds to Kolmogoroff)

$$v_t = v_L \left(\frac{\ell_t}{L}\right)^r \quad , \quad \nu_t = \xi\, v_L\, L \left(\frac{\ell_t}{L}\right)^{r+1} \tag{28}$$

In all practical applications to problems in astrophysics, eq. (28) is actually written as

$$\nu_t = \alpha\, c_s\, H \tag{29}$$

where c_s is the speed of sound and H some characteristic scale height. It is clear that eq. (29) is consistent with (28), *only if* ℓ_t/L is considered a constant of order unity because we limit ourselves to the largest eddies.

Adopting eq. (29), one is then faced with the problem of evaluating the parameter α. The model used by Canuto *et al.* (1985) is based on the equation

$$\varepsilon_{gain} = \varepsilon_{loss} + \varepsilon_{transfer} \tag{30}$$

Here ε_{gain} represents the rate (per unit mass) of energy gain from buoyancy forces and radiation mechanisms; ε_{loss} represents the losses due to heat conduction and molecular viscosity and finally $\varepsilon_{transfer}$ is the energy trans-

ferred by the nonlinear interactions from large eddies to small ones. Since E(k)dk represents the energy in the interval between k and k + dk, one writes, in analogy with the molecular viscosity (Batchelor, 1970)

$$\varepsilon_{transfer} = 2 \nu_t (k) \int_{k_o}^{k} E(k)\, k^2\, dk \tag{31}$$

Let us now consider the growth rate of the unstable modes n(k) derived from the linear analysis. The net rate of energy gain from these modes is obtained by multiplying the average energy of the mode by 2n(k), i.e.

$$\varepsilon_{gain} - \varepsilon_{loss} = 2 \int_{k_o}^{k} n(k)\, E(k)\, dk \tag{32}$$

(Ledoux *et al.*, 1961). The value of ν_t at $k = k_o$ is then easily obtained by combining (31) and (32) with (30). The result is

$$\nu_t = \frac{n(k_o)}{k^2_o} \tag{33}$$

For simplicity, let us approximate the actual geometry of the disc by a plane parallel model with the z-component of k, k_z satisfying the boundary conditions $k_z L = n\pi$ $(n = 1,2,...)$, where $0 \leqslant z \leqslant L$. We have $k_o L = \pi \sqrt{1 + x}$, $x = (k^2_x + k^2_y)/k^2_z$. Using (29) and (33), we then derive

$$\alpha = \frac{1}{\pi^2 (1+x)} \left(\frac{H}{c_s} \right) n(k_o) \left(\frac{L}{H} \right)^2 \tag{34}$$

Eq. (34), providing an expression for α in terms of the ratio between the growth rate $n(k_o)$ and the hydrostatic rate c_s/H, is of general validity regardless of the specific mechanism generating instability.

a) *Convective Turbulence*

In the absence of rotation, the form of n(k) for a plane-parallel geometry is given by (Chandrasekhar, 1961)

$$2n\,(k) = \left\{(\chi - \nu)^2\, k^4 + \frac{4\,\chi\nu}{L^4}\,\mathcal{R}\,\frac{x}{1+x}\right\}^{1/2} - (\chi + \nu)\,k^2 \qquad (35)$$

Here, χ is the thermometric conductivity, ν is the kinematic viscosity, $\mathcal{R}$ is the Raleigh number $= g_* \bar{\alpha}\,\beta\, L^4/\chi\nu$; $\bar{\alpha}$ is the coefficient of thermal expansion and β is the temperature gradient excess over the adiabatic gradient eq. (11); finally, g_* is the z component of gravity ($g_x = g_y = 0$). In the presence of rotation $\vec{\Omega}$ parallel to $\vec{g}$, the function $n(k)$ is given by the solution of the cubic equation (Chandrasekhar, 1961)

$$\frac{L^4}{\nu\chi}\,(n + \chi k^2)\,(n + \nu k^2) = \frac{\mathcal{R}\,x}{1+x}\left[1 - \frac{\sigma T^*}{\mathcal{R}x}\,\frac{n+\chi k^2}{n+\nu k^2}\right] \qquad (36)$$

where $T^* = L^4\Omega^2/\nu^2$ is the Taylor number and $\sigma = \nu/\chi$ is the Prandtl number. For $T^* = 0$, eq. (36) has the solution (35). The last term in eq. (36) represents the effect of Coriolis forces on the perturbations in the velocity and temperature fields.

b) *Application to the Rotating Solar Nebula*

As we have already stated, the horizontal disc is usually taken to be Keplerian, i.e. the gravitational acceleration in the plane of the disc is balanced by the centrifugal force. The only component of gravity that acts on velocity and temperature perturbations is the vertical component g_*, and so the following relations hold

$$g_* = zg/R \quad , \quad dp = -\,g_*\,\rho\,dz \quad , \quad \sigma T^*/\mathcal{R} = \frac{\Omega^2}{g_*\,\bar{\alpha}\beta} = \frac{1}{\bar{\alpha}\beta z} \qquad (37)$$

Eq. (34) can now be written as

$$\alpha = \frac{1}{\pi^2}\,(\bar{\alpha}\beta z)^{1/2}\left(\frac{L}{H}\right)^2 \frac{N}{(1+x)}\left(\frac{H}{c_s}\,\sqrt{\frac{\bar{g}}{R}}\right) \qquad (38)$$

where we have found it convenient to introduce the dimensionless variable

$$N \equiv \frac{n\,(k_o)}{(g_*\,\bar{\alpha}\beta)^{1/2}} \qquad (39)$$

to be chosen as the real, positive part of the solutions of eq. (36), which for $k = k_o$ becomes

$$(N + N_o)(N + \sigma N_o) = \frac{x}{1+x}\left[1 - \frac{\sigma T^*}{\mathcal{R}x}\frac{N + N_o}{N + \sigma N_o}\right], \quad N_o \equiv \frac{(1+x)\ \pi^2}{(\mathcal{R}\sigma)^{1/2}} \tag{40}$$

The evaluation of α is complete once the quantity $\mathcal{R}\sigma$ is expressed in terms of the physical variables of the problem. Since in the case of radiative conduction

$$\mathcal{R}\sigma = \frac{g_* \bar{\alpha}\beta\ L^4}{\chi^2}, \quad \chi \equiv \chi_r \equiv \frac{4acT^3}{3\ k_{op}\ c_p\ \rho^2} \tag{41}$$

where k_{op} is the opacity, we derive (in c.g.s. units)

$$\mathcal{R}\sigma = 1.45\ 10^{33}\left(\frac{M}{M_\odot}\right)(\bar{\alpha}\beta z)\ \frac{(\rho L)^4}{(RT^2)^3}\ c_p^2\ k_{op}^2 \tag{42}$$

Equations (38), (40) and (42) provide the full determination of α, i.e. of ν to be used in eq. (9), $\nu = \nu_t$.

Next, we must determine F_c the convective flux, eq. (11),

$$F_c = c_p\ \rho\ \chi_c\ \beta \tag{43}$$

To that end, we shall adopt a model first proposed by Spiegel (1963) and worked out by Gough (1976), in which the basic ingredient is the growth rate n(k) which, as we have seen, can easily incorporate rotation, eq. (40). Following Gough, with the changes suggested in a later paper, Gough (1978), we derive

$$\chi_c = \frac{A}{1+x}\ \frac{L^2\ n^3\ (k_o)}{g_*\ \bar{\alpha}\beta} = \frac{A}{1+x}\ (\mathcal{R}\sigma)^{1/2}\ N^3\ \chi_r \tag{44}$$

where we have estimated $A = .65$ and χ_r is given by eq. (41).

Eqs. (38) and (44) should be now inserted in eqs. (9) and (11); together with (12), one could then determine the disc structure and then compare the results with those of Lin and his collaborators. The

advantage of such a procedure is that one has fewer free parameters and the possibility of including rotation. This last point may be an important one. In fact, the original Mixing Length Theory was devised for slow rotators like the sun. On the other hand, in the solar nebula the rotation, being Keplerian, is at its maximum and it may therefore play a significant role. The standard MLT can be extended to include rotation at the expense of introducing extra parameters that are then difficult to evaluate. Since the present formalism obviates such difficulties it is important to study the disc structure on this basis (Cabot *et al.*, 1986). It seems clear that the presence of rotation will decrease the value of α, i.e. of ν_t, since from (40) for $\sigma \to 0$ and $\mathcal{R}\sigma \gg 1$

$$N \sim 1 - \frac{\sigma T^*}{\mathcal{R}_X} \tag{45}$$

A smaller ν_t implies a smaller $\dot{M}$, eq. (8), and therefore a longer evolutionary time for the nebula (for a constant Σ).

5. The Formation of the Earth - Standard Scenario

The accretion process that led to the formation of the earth from grains, dust and gas has been studied by several authors (Safronov, 1972; Weidenshilling, 1974, 1976, 1980). For a detailed review, see Wetherill (1980). While early estimates by Schmidt resulted in an accretion time $t_A \approx 250$ m.yrs., recent analyses yield considerably lower values, i.e. $23 \leqslant t_A \leqslant 88$ m.yr. These results assume that accretion occurred in the absence of gas. In the presence of gas (Mizuno *et al.*, 1982; Nakagawa *et al.*, 1981), t_A decreases to about 10 m.yr., and a massive atmosphere ($\sim 10^4$ times the present one or the one corresponding to the gas-free situation) results. Since the two models lead to very different conclusions for the earth's atmosphere, it is important to analyze their basic ingredients. A critical role is played by t_N, the dissipation time of the solar nebula, whose value depends, in most models considered thus far, on the turbulent viscosity $\nu_t = \xi \ell_t v_t$ (where ℓ_t and v_t are typical lengths and velocities of the turhulent motion). A detailed analysis (Elmegreen, 1978; 1979) leads to the following dependence of t_N on ξ

$$t_N = \frac{A}{4\xi} \text{ m.yrs.} \tag{46}$$

where

$$A = (M_N/10^{-1}\ M_\odot)^{1.37}\ (X/50\ AU)^{-1.37}\ (V_W\ \dot{M}_W/2\ 10^{26})^{-1.33} \tag{47}$$

Here, M_N is the mass of the solar nebula, X its extension, V_W the solar wind, and $\dot{M}_W$ the rate of mass loss. The parameter ξ satisfies the following inequalities

$$10^{-3} \leqslant \xi \leqslant 1/3\ , \tag{48}$$

a result arrived at in the following way. As stated earlier, in a turbulent fluid one envisages three regions characterized by different sizes of the eddies there contained. In the first region, the eddies sizes ℓ are comparable with L, the size of the system itself. In this case one writes $\nu = \xi_L\ v\ \ell$, where ξ_L is the inverse of the Reynolds number Re which, for turbulence to set in, must be $> 10^3$, and so $\xi_L < 10^{-3}$, yielding the lower limit in (48). At the other end of the spectrum, the eddies are sufficiently small for molecular forces to dominate, and so $\nu = \xi_m\ v\ \ell$, where $\xi_m = 1/3$, thus yielding the upper unit in (48). Because of the large indeterminacy of (48) Canuto *et al.* (1984) have attempted to calculate ξ from first principles.

One begins by using the Heisenberg-Weizsacker's theory of turbulence (Batchelor, 1970). One has

$$\nu_t\,(k) = \gamma \int_k^\infty \left(\frac{E\,(k)}{k^3}\right)^{1/2} dk\ ,\ v^2_t = \int_k^\infty E\,(k)\,dk\ ,\ \ell_t = \pi/k \tag{49}$$

Here E(k) is the spectral energy distribution function solution of the dynamical equations governing turbulence. Several forms were employed:

1) Kolmogoroff spectrum, $E(k) \sim k^{-5/3}$. In this case

$$\xi = \frac{\gamma}{\pi}\ \sqrt{\frac{3}{8}} = .06\ ,\ \gamma = 1/3 \tag{50}$$

2) The Stewart-Townsend (1951) "experimental" spectrum $E\,(k) \sim k^{-\alpha 2\ \ell n\ k}$. The result is ($\Phi$ (x) is the error function)

$$\xi = \frac{\gamma q}{\pi} \sqrt{\frac{2}{\alpha}} \frac{1 - \Phi(x)}{\{1 - \Phi(y)\}^{1/2}} \tag{51}$$

where $x\sqrt{2} = \alpha \ell nq + .5\,\alpha^{-1}$, $y = \alpha \ell nq - .5\,\alpha^{-1}$, $q = k/k_o = L/\ell$. For a wide range of parameters, the resulting values of ξ are

$$.03 \leqslant \xi < .08 \tag{52}$$

3) In the case of convective turbulence (Ledoux *et al.*, 1961) E(k) cannot be given in closed analytic form. The evaluation of ξ was therefore done numerically. For the range $10^{-7} < \delta < 10^{-1}$ of $\delta = 8\pi^4/\mathcal{R}$, the result is

$$\mathcal{R}\sigma \ll 1 \qquad .03 < \xi < .07 \tag{53}$$

4) The previous theory was extended to the case $\mathcal{R}\sigma \gg 1$. The result is

$$\mathcal{R}\sigma \gg 1 \qquad .06 \leqslant \xi \leqslant .07 \tag{54}$$

Using these results, as well as those of Nakano *et al.* (1979), $\xi = .05$, it was concluded that (Canuto *et al.*, 1984).

$$t_N = (2.5\text{-}8.3)\ 10^6\ A\ \text{yrs} \tag{55}$$

It is interesting to note that for $A = 1$ the upper limit of t_N closely corresponds to the point where the T-Tauri phase (vertical part of the 1 $M_\odot$ track, Fig. 4) ends. Furthermore, since either value of t_N is smaller than the values of t_A, (Wetherill, 1980) it seems unlikely that gas might have influenced accretion to the point of producing a massive H_2 atmosphere. Since the quoted values of t_A, ranging from 10 m.yrs. to (23-88) m.yrs. correspond to extreme assumptions as far as the gas is concerned, our result suggesting a gradual dispersion of the gas while the earth was accreting, would in principle require a new evaluation of t_A with a time decreasing gas density. However, for the present purposes, it is sufficient to take an average of the previous values. If we take $t_A = 50$ m.yrs., we would conclude that the SN gas was present only for 10% of t_A, and that most of the accretion occurred while the sun was moving along the radiative track stage of Fig. 4, at which point the UV flux was 10^2 times larger than its present value.

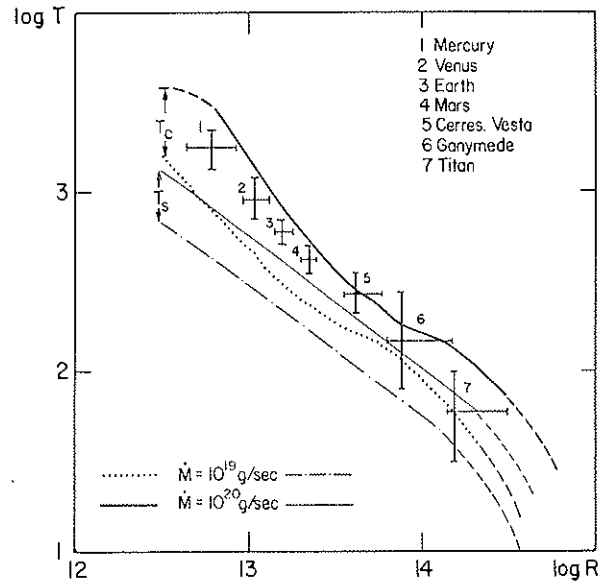

FIG. 3. A comparison of the T vs. R function as deduced from the solutions of Lin and collaborators with those from the work of Lewis. The best fit is achieved for $\dot{M} \cong 10\text{-}6\ M_\odot/yr = 10^{20}$ g sec^{-1}. (Reproduction with permission of Dr. D.N.C. Lin).

As we have stated at the end of Section 3, while this "standard scenario" implies time scales of the order of

$$(10\text{-}50)\ 10^6 \text{ yrs}, \tag{56}$$

Lin's analysis implies time scales shorter by at least a factor of *ten*, thus implying that the Solar UV flux was 10^4 larger than today, as one can see from Figure 4. (For the photochemical implications of high UV fluxes see Section 8).

6. The Origin of the Atmosphere

Since the SN was unlikely the major contributor to the earth's atmosphere, one may consider the following contributors: (1) collision with comets, (2) volatilization of impacting material and (3) outgassing. One may distinguish two periods of outgassing. While the accretion energy due to impact was in principle sufficient to melt the entire Earth, this

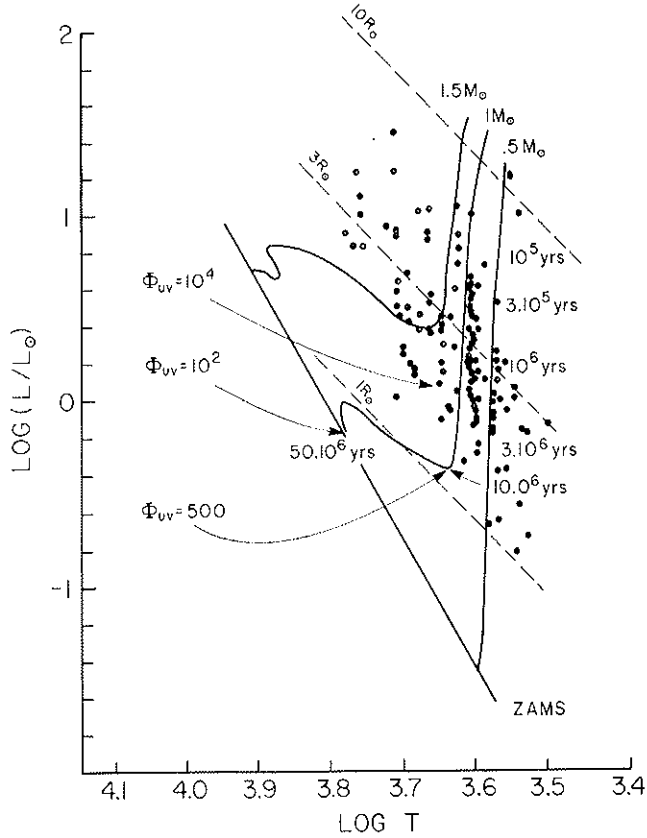

FIG. 4. The pre-main sequence evolution of 0.5 to 1.5 solar mass stars in the Hertzsprung-Russell diagram. The lines represent theoretical evolutionary tracks, while the dots represent observational data for T Tauri stars (Cohen and Kuhi, 1979). The corresponding ages and ratios of UV flux to present solar UV flux are indicated for a solar-mass star.

may not have occurred, since a fully melted Earth would have expelled all volatiles, whilst it is known that He^3 is still degassed today. Accretional heating may have produced partial melting including Fe alloys that migrated toward the center forming ultimately the Earth's core. The time scales for the core formation discussed in the past ($\approx 10^9$ yrs) have been shown to be too long. The conclusion is that the core formed *contemporaneously* with the accretion of the earth itself in $\approx 10^7$ yrs (Stevenson, 1981, 1983). During this period, *two sources of volatiles* therefore acted simultaneously, the outgassing caused by the impacting material that stirred the mantle and

the impacting meteorites. Since volatiles are bound in these meteorites, the energy retained as heat upon impact would be sufficient to vaporize the volatile species releasing them so as to form an atmosphere. As stated by Benlow and Meadows (1977) this conclusion seems unavoidable: the formation *only* of a solid body with the subsequent outgassing seems an artificial division of events which more naturally should be thought of as having occurred simultaneously. As the embryonic Earth continued to grow, the impact velocities increased until vaporization of the impacting material occurred. Non-volatile solids so vaporized cooled and condensed onto the surface. Volatiles like H_2O, CO_2, N_2, the noble gases, etc., probably remained in tbe atmosphere. Calculations by Jakosky and Abrens (1979) indicate that this process occurs for impact velocities greater than 5 km/sec, which in the case of the Earth were achieved (Wetherill, 1976) when the radius was 50% of its present value, i.e. before $\sim 10^6$ yrs.

The chemical composition of this atmosphere depends critically on complex chemical reactions between the infalling vaporized gas, the outgassed volatiles and other elements, particularly Fe (Wetherill, private communication). In the specific impact originated atmosphere studied by Jakosky and Ahrens (1979), the partial pressure of water was estimated to be $p(H_2O) \approx .01$ bar. The fate of atmospheric CO_2 is difficult to quantify and ongoing experiments by Ahrens and collaborators (Stevenson, private communication, 1983) are expected to shed light on this point, since carbonate growth may have removed a great deal of CO_2 during the time scale of the Earth's accretion. The first phase of outgassing, together with an impact-originated atmosphere, lasted a period of time not greatly different from the accretion time itself, at the end of which the Earth entered a period in which accretion is over, the mantle is solid and the core fully formed (Stevenson, 1983). Such a period is characterized by a large "mass flux" which transports large masses of the mantle to the surface region, thus making them available for the second period of outgassing. Since the length of this period is difficult to estimate, the following argument can be made (Thomsen, 1980).

The abundance of $^{129}Xe/^{130}Xe$ in the atmosphere is smaller than that in the solid Earth, the latter being due to enrichment caused by the decay of ^{129}I to ^{129}Xe. If the outgassing took much longer than a few lifetimes of ^{129}I ($17 \cdot 10^6$ yrs), at the end of it there would have been no ^{129}I left and both the atmospheric and the terrestrial ^{129}Xe would have been equally abundant. Since this is not the case, the separation of the ^{129}Xe from the Earth (outgassing), must have occurred while ^{129}I was still present, i.e.

within a few ^{129}I lifetimes, say $50 \cdot 10^6$ yrs. (It must however be pointed out that, as Wetherill has noted, the argument is also consistent with no outgassing of the Earth at all, all the atmospheric ^{129}Xe having perhaps been deposited in the atmosphere by impact).

We therefore conclude that the entire set of phenomena, (1) collapse of the nebula, (2) accretion of the Earth, (3) dissipation of the nebular remnant, (4) formation of the Earth's core, (5) formation of an atmosphere by impact volatiles plus outgassing and finally (6) contribution to the atmosphere by the second outgassing period, may have occurred within 50-100 10^6 yrs, corresponding to the time when the sun entered the main sequence, (Fig. 4).

For our photochemical calculations, Section 8, we have assumed a background composition of the paleoatmosphere consistent with both the impact and outgassing scenarios.

7. Protostars and the Ultraviolet Flux

For a protostar evolving to the main sequence, theoretical models can be used to predict a few observational quantities such as surface temperature and luminosity. However, the models are not sufficient to predict accurately the ultraviolet flux emitted by a pre-main sequence star. Thus we employ ultraviolet observations of young solar-like stars as the best estimate of the UV flux emitted by the young sun.

Observations of pre-main sequence stars indicate that the stars pass through three identifiable stages. During the first stage, the star is still accreting material from its gaseous, dusty environment. The cocoon of dust largely shrouds the star, which is detectable only at infrared and radio wavelengths. Models indicate that a solar-like protostar passes through this stage in about 100 Kyr years (Stahler *et al.*, 1980).

The second stage, which is the best studied, begins as the star becomes visible at visual wavelengths. Several hundred such stars, known as the T Tauri stars, have been identified. The stars still possess an envelope or disk of gas and dust, but it has become thin enough for the stellar surface to be studied. The protostar has become truly "stellar" in structure, possessing a convective interior, a photosphere, and a bright chromosphere. The T Tauri phase is largely defined by the characteristic bright line and continuous emission spectrum, originating primarily in a dense, active chromosphere.

The end of the T Tauri stage can be estimated from the ages of the stars. Ages of 3 to 5 Myr are indicated by the association of the T Tauri

stars with other stars of known ages or from stability arguments (Herbig, 1962; 1970). It has been suggested that the T Tauri phase corresponds to the stage when the protostar's interior is completely convective (Jones and Herbig, 1979). If this is the case, then the theoretical models for stars of various masses may be used to indicate the endpoints of the T Tauri phase. For a solar-mass protostar, the phase would last 10 Myr. More massive stars evolve more quickly; a 2 solar-mass star passes through the phase in 2 Myr. Conversely, a less massive star of 0.7 solar masses passes through the convective phase in 40 Myr. The theoretical predictions of the evolution of a solar-like protostar in the Hertzsprung-Russell diagram are given in Figure 4. Evolutionary tracks for stars of 1.5, 1.0, and 0.5 solar masses are given for comparison. In addition, the time scale for the solar-mass star is indicated. The convective phase of the pre-main sequence evolution corresponds to the vertical portion of the tracks; i.e. the luminosity is decreasing but little change in surface temperature is seen. The change in luminosity is thus largely due to the decreasing radius of the star as it contracts. Superimposed on these evolutionary tracks are observational data for T Tauri stars found in the Taurus-Auriga dark clouds and in the Orion complex (data are from Cohen and Kuhi, 1979). If one compares the observational data and the theoretical tracks, then ages of 100 Kyr to 10 Myr are derived. The overall agreement of all these determinations is good, despite the expected problems of comparing observations of "real stars" to theoretical models. We can conclude, then, that a solar-mass star begins the T Tauri phase of evolution at an age of about 100 Kyr and continues until it is about 6 to 12 Myr of age.

The portion of the star's pre-main sequence evolution following the T Tauri phase comprises about 80% of the time required to reach the main-sequence. Theoretical models indicate that the star's interior develops a radiative core within its convective envelope. During this phase the protostar loses the bright emission and spectral features which make the T Tauri phase so identifiable. As a consequence, these stars, which have been called the post-T Tauri stars, have been found less frequently and are not as well studied. Herbig (1973) originally postulated the probable observational characteristics of the post-T Tauri stars. A handful of these stars have been unexpectedly discovered in recent years by observers using the Einstein X-ray satellite (Feigelson and Kriss, 1981; Walter and Kuhi, 1981). So far the ages of these stars do not appear greatly different from those of the T Tauri stars (Mundt *et al.*, 1983). Therefore clear, observed examples of solar-mass stars with ages of 10 to 50 Myr are lacking.

The sun is a relatively normal star of intermediate mass, temperature and luminosity. It is therefore very reasonable to assume that it once passed through the same three phases of protostellar evolution observed for other stars. This assumption allows us to draw upon ultraviolet observations of young stars to represent the probable ultraviolet spectrum of the young sun.

The brighter T Tauri stars have been observed by various investigators using the International Ultraviolet Explorer (IUE) satellite (Appenzeller *et al.*, 1980; Gahm *et al.*, 1979; Giampapa *et al.*, 1981; Imhoff and Giampapa, 1980; Brown *et al.*, 1981). It is thus possible to derive a reasonable ultraviolet spectrum which is typical of a solar-like star with an age of a few Myr. No IUE observations have been made of the first, infrared stage of a protostar's life. The surrounding dust shell is expected to absorb any ultraviolet radiation emitted by the star. A few observations have been made of the post-T Tauri stars. However, since the evolutionary status of the stars is uncertain and the IUE observations are few, we omit them from further discussion.

We have assembled IUE spectra of three well-observed T Tauri stars to represent a probable ultraviolet spectrum for the very young sun. The three stars, T Tauri, SU Aurigae, and RW Aurigae, represent a range of observational characteristics and thus should provide a reasonable sample of T Tauri ultraviolet spectra. We have reduced fourteen low-resolution IUE spectra of the three stars and formed an average ultraviolet spectrum from about 1225 to 3200 Angstroms. The very important hydrogen Lyman-α emission line is masked in our spectra by geocoronal hydrogen emission. However, a weak stellar feature can be discerned in one of our spectra of RW Aur, superimposed with the geocoronal emission. A rough estimate indicates that the observed stellar Lyman-α emission is about 1/10 the flux of the Balmer-α emission observed in the visible for this star (Kuhi, 1974). If one assumes that the same ratio applies to the other stars, then one would expect much lower Lyman-α fluxes for T Tau and SU Aur. This assumption is consistent with the non-detections of Lyman-α for two of these stars; therefore we adopt this estimate, that the Lyman-α flux is 0.1 times the Balmer-α flux for these stars. We have used published visual fluxes for the stars to complete the wavelength coverage required for the photochemical models (Kuhi, 1974). Small gaps in the ultraviolet and visual data occur where no strong emission lines are expected; therefore simple interpolations were performed for these wavelengths. The average spectrum for the entire range of wavelengths from the ultraviolet

through the visual was formed, corrected for 0.5 magnitudes of visual extinction, and reduced to a distance of 1 AU. The choice of visual extinction was made as a conservative estimate, expected to err on the side of somewhat smaller ultraviolet fluxes, compared to derived values for T Tau, SU Aur, and RW Aur (about 1.4, 0.9, and 0.2 mag respectively).

Figure 5 compares our typical T Tauri spectrum to those of the present sun from 1200 to 7200 Å. The sun, during its T Tauri phase, was more luminous at all wavelengths than it is now. The strong chromospheric lines of hydrogen Lyman-α (1215 Å), the doublet of ionized magnesium (2800 Å), and hydrogen Balmer-α (6563 Å) are clearly seen in the T Tauri-phase spectrum. In Figure 6 we have converted the T Tauri-phase and present solar fluxes to units of photons per bin, as used in our photochemical code. The discontinuity at 6500 Å reflects a change in the bin size. Figure 7 shows the ratio of the T Tauri-phase fluxes to the present solar fluxes, using a logarithmic scale. The enhancement of the ultraviolet fluxes, which are very important in many photochemical processes, becomes obvious in this figure. The far-ultraviolet fluxes during the T Tauri phase were up to 10,000 times those currently observed for the sun. This result agrees with the rougher estimate given in our previous paper (Canuto *et al.*, 1982).

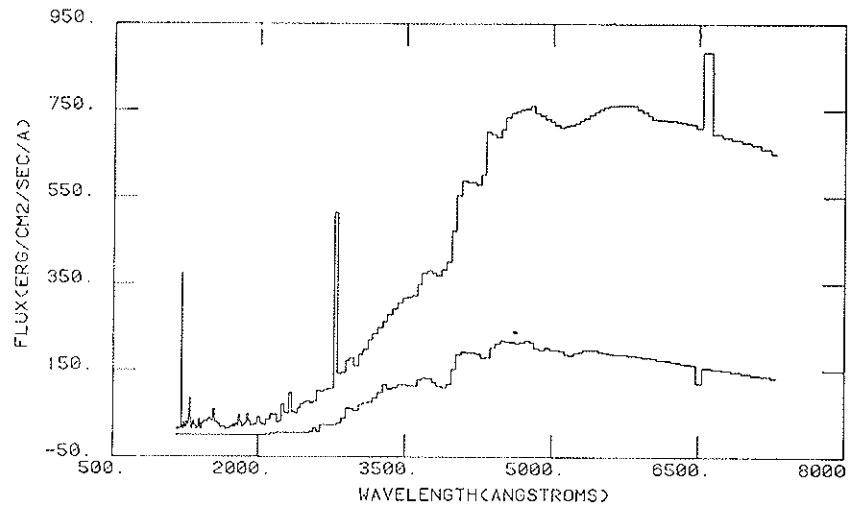

FIG. 5. The T Tauri-phase fluxes (top) compared to present solar fluxes (Ackermann, 1971) for ultraviolet and visual wavelengths. The strong emission lines of Lyman-α (1215 Å), MgII (2800 Å) and Balmer-α (6563 Å) can be seen in the T Tauri spectrum. Fluxes have been reduced to those intercepted at a distance of 1 AU from the star.

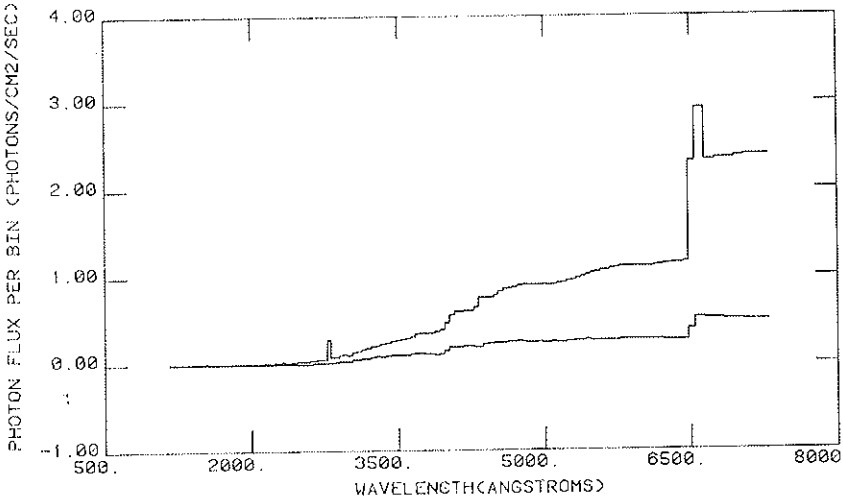

FIG. 6. T Tauri-phase and present solar fluxes converted to photons per bin, as required by the photochemical code. The discontinuity near 6500 Å represents a change in the bin size.

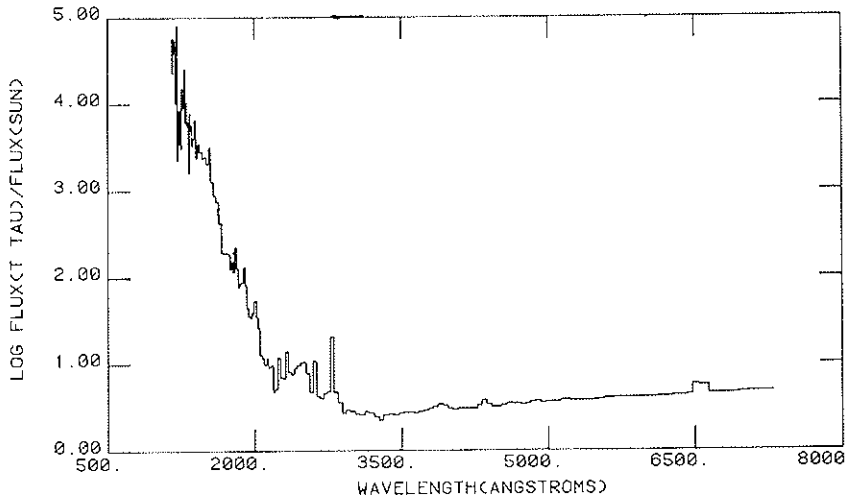

FIG. 7. The ratio of T Tauri-phase fluxes to the present solar fluxes, using a logarithmic scale. Although the enhancement of the T Tauri over the solar fluxes is seen at all wavelengths, it is the most dramatic in the far-ultraviolet.

The enhancement of the T Tauri-phase ultraviolet flux over the present sun's fluxes is clearly very wavelength-dependent (see also Table 1). Thus use of this average T Tauri spectrum should represent a significant improvement to our wavelength-independent treatment used previously as input for the photochemical models (Canuto *et al.*, 1982).

The T Tauri phase represents a very early stage in the evolution of a solar-like protostar. Is it possible to estimate what changes occur to the ultraviolet spectrum during the 80% of the protostar's life after the T Tauri phase? A study of the variation of the ultraviolet emission lines with age has been performed for young main-sequence stars (Boesgaard and Simon, 1982). They find that the emission line fluxes decrease as $t^{-1/2}$ (although some of the higher temperature lines may fall off more rapidly). If this is the case for stars which have not yet reached the main sequence, then we can estimate the overall decrease in the ultraviolet fluxes with time after the T Tauri phase (see Table 2 in Canuto *et al.*, 1982). We find that the far-ultraviolet luminosity of the sun when it reached the main sequence was 100 times its present value. Thus with some small caveats the results obtained here for the T Tauri stars may be applied to the later stages of the sun's pre-main sequence evolution.

8. The Photochemistry of Oxygen, Ozone, and Formaldehyde in the Early Atmosphere

In the prebiological early atmosphere, the photolysis of water vapor (H_2O) and carbon dioxide (CO_2) led to the photochemical production of

Table 1 - Solar energy flux averaged over the Earth during T-Tauri phase (Values in parentheses correspond to today).

Source	Energy (cal cm^{-2} yr^{-1})
Total Radiation	$4.6\ 10^6$ ($.26\ 10^6$)
UV light	
< 3000 Å	$2.4\ 10^4$ ($.34\ 10^4$)
< 2500 Å	$9.9\ 10^3$ ($.56\ 10^3$)
< 2000 Å	$5.0\ 10^3$ (40)
< 1500 Å	$2.2\ 10^3$ (1.7)

three biologically-significant species: molecular oxygen (O_2), ozone (O_3), and formaldehyde (H_2CO). Oxygen is important due to its detrimental effects on the origin and evolution of life; i.e., laboratory chemical evolution experiments cannot proceed to the synthesis of complex organic molecules in the presence of free oxygen above trace levels. Ozone, a photochemical product of oxygen, absorbs solar ultraviolet (UV) radiation between 200 and 300 nm and eventually shielded the Earth's surface from this biologically lethal radiation. Formaldehyde was a key molecule in the process of chemical evolution — that is the formation of complex organic molecules. In the present atmosphere, H_2CO is a trace species photochemically produced via the methane (CH_4) oxidation chain (for example, see Levine and Allario, 1982) with the precursor CH_4 being produced via biogenic activity. However, because the lifetime of CH_4 in the prebiological atmosphere was extremely short due to photochemical destruction, if it was present at all (Levine *et al.*, 1982), the question then arises as to how to produce H_2CO in the absence of CH_4. A prebiological photochemical source for H_2CO initiated by the photolysis of H_2O and CO_2 has been suggested by Pinto *et al.* (1980). The photochemical and chemical processes leading to the production of O_2, O_3, and H_2CO in the prebiological atmosphere will be summarized and then theoretical calculations obtained with a one-dimensional photochemical of the prebiological paleo-atmosphere will be discussed.

The photochemical production of O_2, O_3, and H_2CO is initiated by the photolysis of H_2O and CO_2:

(1) $H_2O + h\nu \rightarrow OH + H$ ($\lambda \leqslant 240$ nm), and
(OH = hydroxyl radical; H = atomic hydrogen)

(2) $CO_2 + h\nu \rightarrow CO + O$ ($\lambda < 230$ nm)
(CO = carbon monoxide; O = atomic oxygen)

Reaction (1) leads to the production of oxygen atoms (O) through:

(3) $OH + OH \rightarrow O + H_2O$

The oxygen atoms formed in reactions (2) and (3) form molecular oxygen (O_2) through the following reactions:

(4) $O + O + M \rightarrow O_2 + M$

(5) $O + OH \rightarrow O_2 + H$

The destruction of O_2 is controlled by its photolysis (6) and its chemical reaction with H_2

(6) $O_2 + h\nu \rightarrow O + O$, $\lambda \leqslant 242$ nm, and

(7) $2\,H_2 + O_2 \rightarrow 2\,H_2O$. (Net Cycle)

Closely coupled to the origin and evolution of O_2 is the origin and evolution of O_3. O_3 is photochemically produced through the reaction:

(8) $O + O_2 + M \rightarrow O_3 + M$

O_3 is photochemically destroyed through direct photolysis (9), reaction with O (10), and through a series of catalytic cycles involving the oxides of nitrogen, hydrogen, and chlorine:

(9) $O_3 + h\nu \rightarrow O_2 + O$, $\lambda \leqslant 1100$ nm, and

(10) $O_3 + O \rightarrow 2\,O_2$.

The photochemical production of H_2CO proceeds with reaction H and CO formed in (1) and (2), leading to the formation of the formyl radical (HCO):

(11) $H + CO + M \rightarrow HCO + M$.

The reaction between two HCO radicals forms H_2CO:

(12) $HCO + HCO \rightarrow H_2CO + CO$

The radical is photochemically destroyed by direct photolysis (13) and by reactions with O, H, OH, O_2, and HO_2 (hydroperoxyl radical) (14) through (19):

(13) $HCO + h\nu \rightarrow H + CO$

(14) $HCO + O \rightarrow H + CO_2$

(15) $HCO + O \rightarrow OH + CO$

(16) $HCO + H \rightarrow H_2 + CO$

(17) $HCO + OH \rightarrow H_2O + CO$

(18) $HCO + O_2 \rightarrow HO_2 + CO$

(19) $HCO + HO_2 \rightarrow H_2O_2 + CO$
(H_2O_2 = hydrogen peroxide).

H_2CO is photochemically destroyed through direct photolysis (20) and (21) and by reactions with O, H, and OH:

(20) $H_2CO + h\nu \rightarrow H + HCO,\ 278 \leqslant \lambda \leqslant 327$ nm

(21) $H_2CO + h\nu \rightarrow H_2 + CO,\ 278 \leqslant \lambda \leqslant 327$ nm

(22) $H_2CO + O \rightarrow OH + HCO$

(23) $H_2CO + H \rightarrow H_2 + HCO$

(24) $H_2CO + OH \rightarrow HCO + H_2O$

Once photochemically formed in the early atmosphere via reactions (1), (2), (11), and (12), H_2CO, being very water soluble, rained out of the atmosphere. In the early oceans, H_2CO accumulated and eventually underwent aqueous solution polymerization reactions leading to the abiotic synthesis of organic molecules of increasing complexity (Pinto *et al.*, 1980).

We have calculated the vertical distributions of O_2, O_3, and H_2CO as well as O, CO, H, OH, HO_2, and H_2O_2 by simultaneous solution of reactions (1) to (24), along with other reactions that govern the chemical transformations of the hydrogen species (H, OH, HO_2, and H_2O_2). The total reaction scheme includes nine photochemical processes, 37 chemical processes, and the rainout loss of the water-soluble species (H_2CO and H_2O_2). These photochemical, chemical, and rainout processes and their reaction rates are summarized in Table 2. In our calculations, we have assumed that molecular nitrogen (N_2), at a partial pressure of 0.8 bar, is the major atmospheric constituent. N_2 is a chemically-inert gas that participates in chemical reactions only as a third body (M). The H_2O vapor mixing ratio is specified in the troposphere (surface to 14.5 km) and varies from 1.2×10^{-2} at the surface to 4.6×10^{-7} at 14.5 km (the tropopause in the model). Above the tropopause, the distribution of H_2O vapor is calculated as a chemically-active species using a continuity/transport equation for H_2O. Because of the lack of information concerning the level of CO_2 in the prebiological paleoatmosphere, we have performed theoretical calculations for two different values: the pre-industrial level of

TABLE 2 - Photochemical and Chemical Reactions.

Reaction Number	Reaction	Rate Constant* (sec^{-1}, cm^3 sec^{-1} or cm^6 sec^{-1})	
J1:	$O_2 + h\nu \rightarrow O + O$	4.7×10^{-10}	6.3×10^{-9}
J2:	$O_3 + h\nu \rightarrow O + O_2$	2.2×10^{-4}	8.5×10^{-4}
J3:	$O_3 + h\nu \rightarrow O(^1D) + O_2$	4.4×10^{-3}	2.8×10^{-2}
J4:	$H_2O + h\nu \rightarrow OH + H$	1.1×10^{-14}	5.1×10^{-13}
J5:	$H_2O_2 + h\nu \rightarrow OH + OH$	5.3×10^{-5}	4.4×10^{-4}
J6:	$H_2CO + h\nu \rightarrow H + HCO$	4.8×10^{-5}	1.6×10^{-4}
J7:	$H_2CO + h\nu \rightarrow H_2 + CO$	4.9×10^{-5}	1.4×10^{-4}
J8:	$CO_2 + h\nu \rightarrow CO + O$	1.3×10^{-12}	6.3×10^{-11}
J9:	$HCO + h\nu \rightarrow H + CO$	1.3×10^{-2}	5.8×10^{-2}
1	$O + O_2 + M \rightarrow O_3 + M$	1.1×10^{-34}	exp (510/T)
2	$O + O_3 \rightarrow 2O_2$	1.5×10^{-11}	exp(−2218/T)
3	$O(^1D) + O_2 \rightarrow O + O_2$	3.2×10^{-11}	exp (67/T)
4	$O(^1D) + N_2 \rightarrow O + N_2$	2.0×10^{-11}	exp (107/T)
5	$H_2O + O(^1D) \rightarrow 2OH$	2.3×10^{-10}	
6	$H + O_2 + M \rightarrow HO_2 + M$	2.1×10^{-32}	exp (290/T)
7	$H + O_3 \rightarrow OH + O_2$	1.4×10^{-10}	exp (−470/T)
8	$OH + O \rightarrow H + O_2$	4.0×10^{-11}	
9	$OH + O_3 \rightarrow HO_2 + O_2$	1.6×10^{-12}	exp (−940/T)
10	$OH + OH \rightarrow H_2O + O$	1.0×10^{-12}	exp (−500/T)
11	$HO_2 + O \rightarrow OH + O_2$	3.5×10^{-11}	
12	$HO_2 + O_3 \rightarrow OH + 2O_2$	1.1×10^{-14}	exp (−580/T)
13	$HO_2 + OH \rightarrow H_2O + O_2$	4.0×10^{-11}	
14	$HO_2 + HO_2 \rightarrow H_2O_2 + O_2$	2.5×10^{-12}	
15	$H_2O_2 + OH \rightarrow HO_2 + H_2O$	1.0×10^{-11}	exp (−750/T)
16	$O(^1D) + H_2 \rightarrow OH + H$	9.9×10^{-11}	
17	$OH + OH + M \rightarrow H_2O_2 + M$	See JPL Publication 82-57 (1982)	
18	$H_2O_2 + O \rightarrow OH + HO_2$	2.8×10^{-12}	exp(−2125/T)
19	$H_2 + OH \rightarrow H_2O + H$	1.2×10^{-11}	exp(−2200/T)
20	$H_2CO + OH \rightarrow HCO + H_2O$	1.7×10^{-11}	exp(−100/T)
21	$H_2CO + O \rightarrow OH + HCO$	2.8×10^{-11}	exp(−1540/T)
22	$HCO + O_2 \rightarrow CO + HO_2$	5.0×10^{-12}	
23	$CO + OH \rightarrow H + CO_2$	See JPL Publication 82-57 (1981)	

* Photolysis rates (sec^{-1}) for H_2 = 17 ppmv are given for UV = 1 (first value) and UV = T-Tauri phase.

TABLE 2 - (Continued).

Reaction Number	Reaction	Rate Constant (sec^{-1}, $cm^3\ sec^{-1}$ or $cm^6\ sec^{-1}$)
24	$O + O + M \rightarrow O_2 + M$	2.8×10^{-34} exp (710/T)
25	$H + H + M \rightarrow H_2 + M$	8.3×10^{-33}
26	$H_2 + O \rightarrow OH + H$	3.0×10^{-14} exp(−4480/T)
27	$H + HO_2 \rightarrow O_2 + H_2$	4.7×10^{-11} (×0.29)
28	$H + HO_2 \rightarrow H_2O + O$	4.7×10^{-11} (×0.02)
29	$H + HO_2 \rightarrow OH + OH$	4.7×10^{-11} (×0.69)
30	$H + CO + M \rightarrow HCO + M$	2.0×10^{-33} exp(−850/T)
31	$H + HCO \rightarrow H_2 + CO$	3.0×10^{-10}
32	$HCO + HCO \rightarrow H_2CO + CO$	6.3×10^{-11}
33	$OH + HCO \rightarrow H_2O + CO$	5.0×10^{-11}
34	$O + HCO \rightarrow H + CO_2$	1.0×10^{-10}
35	$O + HCO \rightarrow OH + CO$	1.0×10^{-10}
36	$HO_2 + HCO \rightarrow H_2O_2 + CO$	1.0×10^{-11}
37	$H_2CO + H \rightarrow H_2 + HCO$	2.8×10^{-11} exp(−1540/T)
38	H_2CO and H_2O_2 rainout	1.0×10^{-6} s^{-1}

280 ppmv (CO_2 = 1) and for 100 times this value (CO_2 = 100). We have also added trace volcanic gases — molecular hydrogen (H_2) and carbon monoxide (CO) — in our model. Calculations were performed for two values of H_2 surface mixing ratio: 17 ppmv (Kasting and Walker, 1981) and 10^{-3} (Pinto *et al.*, 1980). The surface volcanic flux of CO was taken to be 2×10^8 molecules $cm^{-2}\ s^{-1}$ (Kasting and Walker, 1981). Methane and ammonia were not included as constituents of the prebiological paleoatmosphere for reasons discussed in Levine (1982) and Levine *et al.* (1982). The U.S. Standard Atmosphere Mid-Latitude Spring/Autumn temperature profile is specified in the troposphere. An early atmosphere temperature profile for the O_3-deficient stratosphere that decreases linearly from the tropopause to the mesopause is used. This profile is based on coupled photochemical-radiative equilibrium temperature calculations (Levine and Boughner, 1979). Photodissociation rates are diurnally averaged for a latitude of 30° and solar declination of 0° (Rundel, 1977). The model includes the solar spectrum from 110 to 735 nm (Ackermann, 1971). We have performed calculations for the present ultraviolet flux (UV = 1)

(Ackermann, 1971) and for two additional values: 300 times the present value and for the wavelength-dependent ultraviolet flux emitted by early sun-like stars (T-Tauri) as observed with the International Ultraviolet Explorer (IUE) satellite (Canuto *et al.*, 1982, and Canuto *et al.*, 1983). The model extends from the surface to 53.5 km with 1 kilometer spatial resolution between the surface and 10 km, and 1.5 kilometers spatial resolution between 10 and 53.5 km. Further details about the model are given in Levine *et al.* (1981) and Levine *et al.* (1982).

a) *Results*

The effects of H_2 on the calculated vertical distribution of O_2 for preindustrial levels of CO_2 (280 ppmv) for three different values of solar ultraviolet radiation (UV): 1,300, and the T-Tauri flux, are shown in Figure 8 (for H_2 = 17 ppmv) and Figure 9 (for $H_2 = 10^{-3}$). We found higher O_2 levels for lower values of H_2. This is not surprising since higher values of H_2 result in the more rapid loss of O_2 due to the reformation of H_2O (reaction (7)). For H_2 = 17 ppmv, the surface O_2 mixing ratio increased from 10^{-14} to 10^{-11} as the solar UV flux was increased. For $H_2 = 10^{-3}$, the surface O_2 mixing ratio increased from 10^{-17} to almost 10^{-13} for the same increase in the UV flux.

The effects of H_2 on the calculated vertical distribution of O_2 for enhanced levels of CO_2 (100 times the pre-industrial level, corresponding

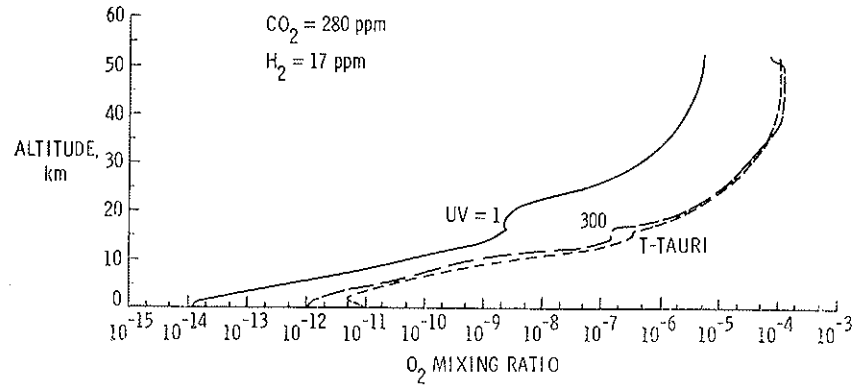

FIG. 8. Vertical distribution of molecular oxygen (O_2) mixing ratio in prebiological paleoatmosphere. Calculations for molecular hydrogen (H_2) = 17 ppmv, carbon dioxide (CO_2) = 280 ppmv, and three different solar ultraviolet fluxes.

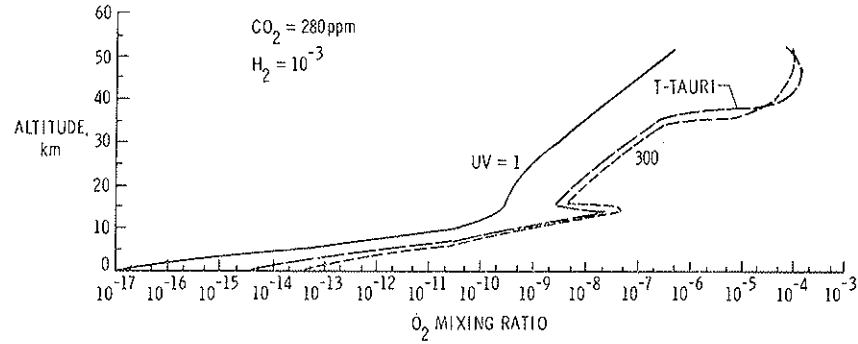

FIG. 9. Vertical distribution of molecular oxygen (O_2) mixing ratio in prebiological paleoatmosphere. Calculations for molecular hydrogen (H_2) = 10^{-3}, carbon dioxide (CO_2) = 280 ppmv, and three different solar ultraviolet fluxes.

to a mixing ratio of 2.8×10^{-2} or 0.028 or 2.8 percent by volume) for three different values of solar UV flux are shown in Figure 10 (H_2 = 17 ppmv) and Figure 11 ($H_2 = 10^{-3}$). For H_2 = 17 ppmv, the surface O_2 mixing ratio increased from less than 10^{-10} to more than 10^{-9} (several parts per billion by volume) as the UV flux was increased. The calculations

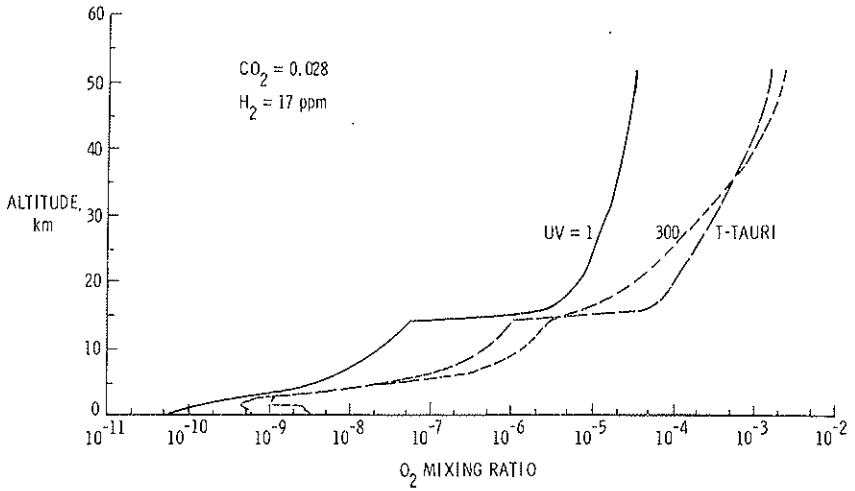

FIG. 10. Vertical distribution of molecular oxygen (O_2) mixing ratio in prebiological paleoatmosphere. Calculations for molecular hydrogen (H_2) = 17 ppmv, carbon dioxide (CO_2) = 0.028, and three different solar ultraviolet fluxes.

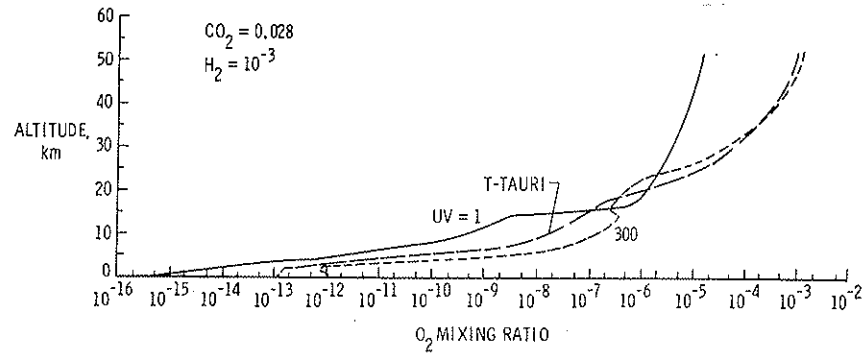

FIG. 11. Vertical distribution of molecular oxygen (O_2) mixing ratio in prebiological paleoatmosphere. Calculations for molecular hydrogen (H_2) = 10^{-3}, carbon dioxide (CO_2) = 0.028, and three different solar ultraviolet fluxes.

shown in this figure represent our maximum calculated levels of O_2. For $H_2 = 10^{-3}$, the surface O_2 mixing ratio increased from 10^{-15} to 10^{-12} (parts per trillion hy volume) as the UV flux was increased.

Surface concentrations of O_2, as well as O_3, H_2CO, O, OH, CO, H, and HCO as a function of H_2, CO, and solar UV levels, are summarized in Table 3.

The effects of H_2, CO_2, and UV levels on the calculated distribution of O_3 corresponding to the previous four O_2 calculation figures are shown in Figures 12-15. Figures 12 and 13 are for the pre-industrial level of CO_2. For $H_2 = 17$ ppmv (Figure 12), the surface number density of O_3 increased from less than 10 to more than 10^3 molecules cm^{-3} as the solar UV was increased. For $H_2 = 10^{-3}$ (Figure 13), the surface number density of O_3 increased from less than 10^{-4} to more than 10^{-1} molecules cm^{-3} as the solar UV was increased. Figures 14 and 15 are for enhanced levels of CO_2 ($CO_2 = 0.028$). For $H_2 = 17$ ppmv (Figure 14), the surface number density of O_3 increased from 10^5 to 10^7 molecules cm^{-3} as the solar UV was increased. For $H_2 = 10^{-3}$ (Figure 15), the surface number density of O_3 increased from 10^{-1} to 10^2 molecules cm^{-3} as the solar UV was increased.

For O_3 shielding considerations, the total atmospheric burden or column density of O_3 (molecules cm^{-2}) above the surface is a more relevant quantity. The column density represents the integral over the O_3 profiles given in Figures 12-15. The O_3 column density as a function of H_2, CO_2, and solar UV levels is summarized in Table 4. Even though certain com-

TABLE 3 - Surface concentration of several species (cm^{-3}) as a function of UV flux and CO_2 and H_2 level.

	I. H_2 = 17 ppm			
	UV = 1		UV = T-Tauri phase	
Species	CO_2 = 1	CO_2 = 100	CO_2 = 1	CO_2 = 100
O	8.95 (6)	4.47 (7)	4.92 (8)	1.96 (9)
O_2	2.72 (5)	1.36 (9)	2.33 (7)	1.29 (10)
O_3	5.66	1.69 (5)	2.20 (3)	1.46 (7)
OH	4.13 (3)	1.51 (4)	2.28 (5)	6.66 (5)
CO	5.09 (11)	7.86 (13)	1.10 (11)	5.16 (13)
H	3.24 (7)	4.09 (6)	1.36 (9)	1.28 (8)
HCO	1.39 (6)	2.06 (7)	5.58 (5)	2.50 (7)
H_2CO	1.62 (6)	2.65 (8)	3.38 (4)	7.17 (7)
CO/CO_2	9.02 (−5)	1.39 (−4)	1.95 (−5)	9.15 (−5)
	II. H_2 = 10^{-3}			
O	2.10 (5)	6.57 (6)	9.49 (6)	1.44 (8)
O_2	1.87 (2)	1.20 (4)	6.12 (4)	1.99 (6)
O_3	1.07 (−4)	2.21 (−1)	2.18 (−1)	1.15 (2)
OH	7.64 (1)	2.60 (2)	3.67 (3)	1.45 (4)
CO	3.09 (13)	3.63 (15)	2.66 (13)	2.37 (15)
H	3.46 (6)	2.32 (5)	4.34 (7)	8.60 (6)
HCO	1.50 (7)	7.95 (7)	3.26 (7)	3.55 (8)
H_2CO	4.14 (8)	4.12 (9)	3.79 (8)	2.43 (10)
CO/CO_2	5.48 (−3)	6.44 (−3)	4.72 (−3)	4.20 (−3)

binations of H_2, CO_2, and solar UV flux result in O_3 column densities as high as 10^{16} molecules cm^{-2}, this is still significantly below the value needed for shielding of the surface from solar ultraviolet radiation of about 6×10^{18} molecules cm^{-2}. The present O_3 column density, which varies with latitude and season, is about 1×10^{19} molecules cm^{-3}. Therefore, we conclude that prehiological levels of O_3 offered no shielding of the surface from biologically lethal solar ultraviolet radiation (200-300 nm). The problem of shielding is further complicated by the enhanced levels of ultraviolet radiation that the early sun may have emitted (Canuto *et al.*, 1982; Canuto *et al.*, 1983).

The effects of H_2, CO_2, and solar UV flux on the vertical distribution of H_2CO are summarized in Figure 16 (H_2 = 17 ppmv) and Figure 17

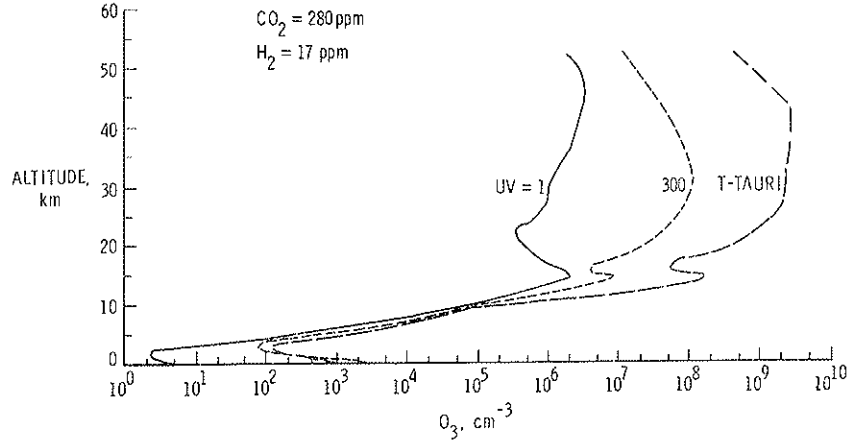

FIG. 12. Vertical distribution of ozone (O_3) concentration (molecules cm^{-3}) in prebiological paleoatmosphere. Calculations for molecular hydrogen (H_2) = 17 ppmv, carbon dioxide (CO_2) = 280 ppmv, and three different solar ultraviolet fluxes.

($H_2 = 10^{-3}$). For H_2 = 17 ppmv, the H_2CO profiles exhibited a range of surface concentrations from 10^4 to 10^8 molecules cm^{-3} as the CO_2 and solar UV flux were increased. For $H_2 = 10^{-3}$, the profiles exhibited a more constant value of between 10^9 and 10^{10} molecules cm^{-3} as the CO_2 and solar UV flux were increased. Maximum surface H_2CO number densities corresponded to the high H_2 cases (10^{-3}).

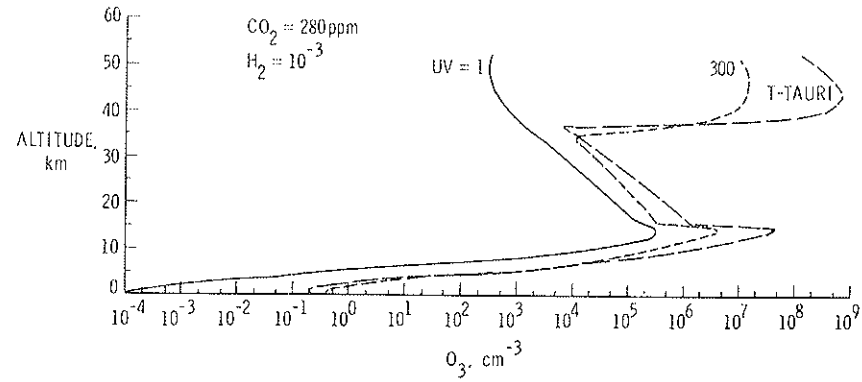

FIG. 13. Vertical distribution of ozone (O_3) concentration (molecules cm^{-3}) in prebiological paleoatmosphere. Calculations for molecular hydrogen (H_2) = 10^{-3}, carbon dioxide (CO_2) = 280 ppmv, and three different solar ultraviolet fluxes.

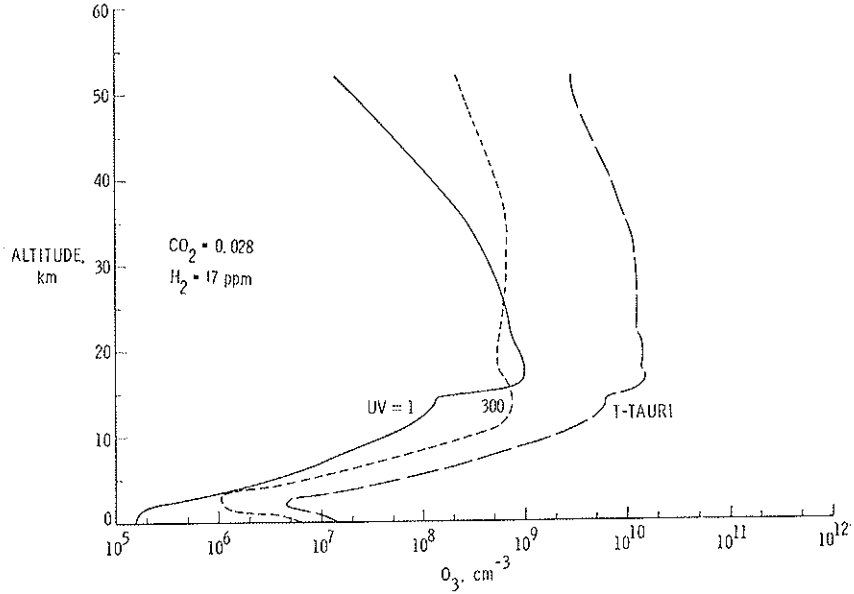

FIG. 14. Vertical distributions of ozone (O_3) concentration (molecules cm^{-3}) in prebiological paleoatmosphere. Calculations for molecular hydrogen (H_2) = 17 ppmv, carbon dioxide (CO_2) = 0.028, and three different solar ultraviolet fluxes.

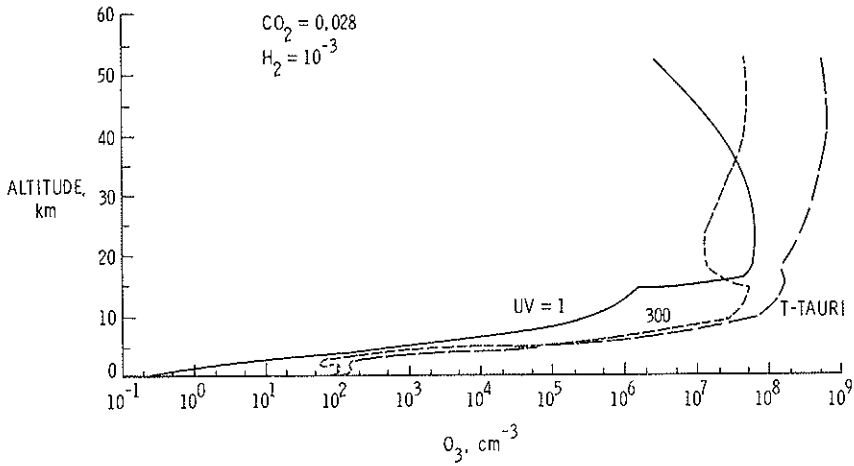

FIG. 15. Vertical distribution of ozone (O_3) concentration (molecules cm^{-3}) in prebiological paleoatmosphere. Calculations for molecular hydrogen (H_2) = 10^{-3}, carbon dioxide (CO_2) = 0.028, and three different solar ultraviolet fluxes.

TABLE 4 - Column Densities of O_3 and H_2CO (molecules cm^{-2}).

	O_3			
	UV = 1		UV = T-Tauri phase	
	$CO_2 = 1$	$CO_2 = 100$	$CO_2 = 1$	$CO_2 = 100$
$H_2 = 17$ ppmv	3.3(12)	1.5 (15)	7.4(15)	4.05(16)
$H_2 = 10^{-3}$	2.1(11)	1.3 (14)	6.5(14)	2.01(15)
	H_2CO			
$H_2 = 17$ ppmv	5.4(11)	7.34(13)	5.9(9)	5.45(13)
$H_2 = 10^{-3}$	8.6(14)	2.02(15)	3.7(14)	1.1 (16)

To calculate the rainout rate of H_2CO, the total atmospheric burden or column density (molecules cm^{-2}) must be known. The H_2CO column density as a function of H_2, CO_2, and solar UV flux levels is summarized in Table 4. The surface production and loss rates, including the loss due to rainout of H_2CO as a function of H_2, CO_2, and solar UV levels, are summarized in Table 5. The last entries in this table summarize the rainout fluxes of H_2CO (molecules cm^{-2} sec^{-1}). The rainout flux is the product

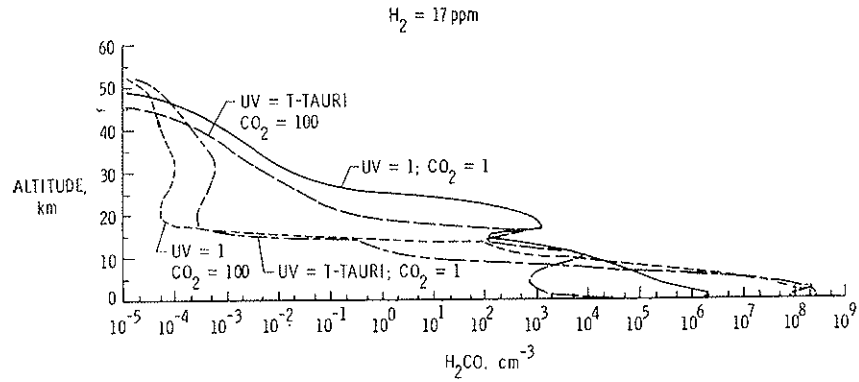

FIG. 16. Vertical distribution of formaldehyde (H_2CO) concentration (molecules cm^{-3}) in prebiological paleoatmosphere. Calculations for molecular hydrogen (H_2) = 17 ppmv and four different combinations of carbon dioxide (CO_2 = 1 and 100) and solar ultraviolet radiation (UV = 1 and T-Tauri).

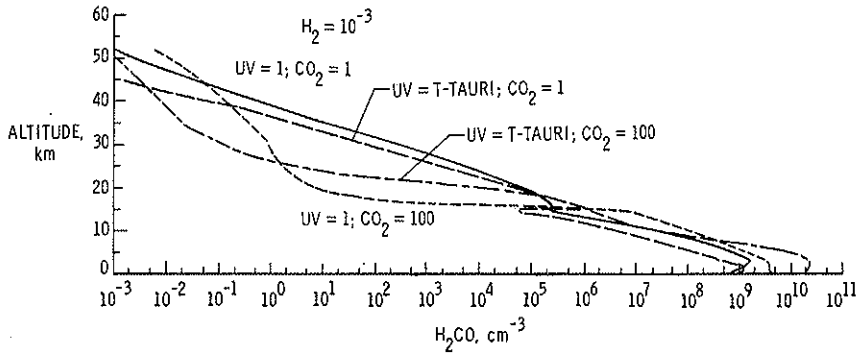

FIG. 17. Vertical distribution of formaldehyde (H_2CO) concentration (molecules cm^{-3}) in prebiological paleoatmosphere. Calculations for molecular hydrogen (H_2) = 10^{-3} and for four different combinations of carbon dioxide (CO_2 = 1 and 100) and solar ultraviolet radiation (UV = 1 and T-Tauri).

TABLE 5 - Surface Production and Loss Rates for H_2CO as a function of UV flux and CO_2 level (H_2 = 17 ppmv).

	Reaction	Reaction Rate (molecules cm^{-3} s^{-1})			
		UV = 1		UV = T-Tauri	
		CO_2=1	CO_2=100	CO_2=1	CO_2=100
1.	Production				
(4)	$HCO + HCO \rightarrow H_2CO + CO$	1.22 (2)	2.67 (4)	1.97 (1)	3.93 (4)
2.	Loss due to photochemistry/chemistry				
	$H_2CO + h\nu \rightarrow H + HCO$	7.75 (1)	1.26 (4)	5.35 (0)	1.05 (4)
	$H_2CO + h\nu \rightarrow H_2 + CO$	7.97 (1)	1.30 (4)	4.84 (0)	9.86 (3)
	$H_2CO + H \rightarrow H_2 + HCO$	7.03 (0)	1.45 (2)	6.16 (0)	1.22 (3)
	$H_2CO + OH \rightarrow HCO + H_2O$	8.04 (−2)	4.81 (1)	9.26 (−2)	5.74 (2)
	$H_2CO + O \rightarrow OH + HCO$	1.94 (0)	1.58 (3)	2.22 (0)	1.88 (4)
	Total:	1.66 (2)	2.74 (4)	1.87 (1)	4.10 (4)
3.	Loss due to rainout (cm^{-3} sec^{-1})	1.62	2.65 (2)	3.38 (−2)	7.17 (1)
4.	Rain-out rate (cm^{-2} sec^{-1})				
	H_2 = 17 ppmv	5.5 (5)	7.34 (7)	5.98 (3)	5.45 (7)
	$H_2 = 10^{-3}$	8.6 (8)	2.02 (9)	3.7 (8)	1.07 (10)

of the column density of H_2CO, summarized in Table 4, and the rainout loss coefficient, which has a value of 10^{-6} sec^{-1} (11.6 days).

The effects of H_2, CO_2, and solar UV on the vertical distribution of the ratio of CO/CO_2 are shown in Figures 18 (H_2 = 17 ppmv) and 19 ($H_2 = 10^{-3}$). The value of the ratio of CO/CO_2 has recently been identified as a key parameter in laboratory experiments dealing with the abiotic synthesis of complex organic molecules in mildly reducing early atmospheric mixtures of N_2, H_2O, CO_2, and CO (Bar-Nun and Chang, 1983). The calculated ratio of CO/CO_2 in the lower atmosphere exhibited a strong dependence on the level of H_2. For H_2 = 17 ppmv, this ratio was about 10^{-4} for various combinations of CO_2 and solar UV flux, while for $H_2 = 10^{-3}$, this ratio was considerably more — about 10^{-2} for the same combination of CO_2 and solar UV flux. However, for either value of H_2, a ratio of CO/CO_2 of unity or greater was reached above about 40 km. The surface ratio of CO/CO_2 as a function of H_2, CO_2, and UV levels is summarized in Table 3.

b) *Summary of the photochemical results*

1. Calculated concentrations of O_2, O_3, and H_2CO, and the ratio of CO/CO_2 in the prebiological paleoatmosphere are very sensitive to atmospheric levels of H_2O and CO_2 and to the flux of incident solar ultraviolet. At least two of these parameters (CO_2 and solar UV) may have varied significantly over geological time.

2. For high levels of CO_2 (100 times the pre-industrial level of 280 ppmv) and solar UV, surface levels of O_2 may have approached the parts per billion (10^{-9}) level in the prebiological paleoatmosphere.

3. Prebiological levels of O_3 offered no shielding of the surface to incoming solar ultraviolet radiation (200-300 nm).

4. Enhanced levels of H_2CO could have been photochemically produced in the atmosphere for high levels of CO_2 and solar ultraviolet flux. On the order of 10 percent or more of the total production of H_2CO may have been rained out of the atmosphere into the early oceans where they could have been synthesized into more complex organic molecules by polymerization reactions.

5. Values of CO/CO_2 of greater than unity were possible for enhanced levels of solar UV flux. Values of this ratio greater than unity

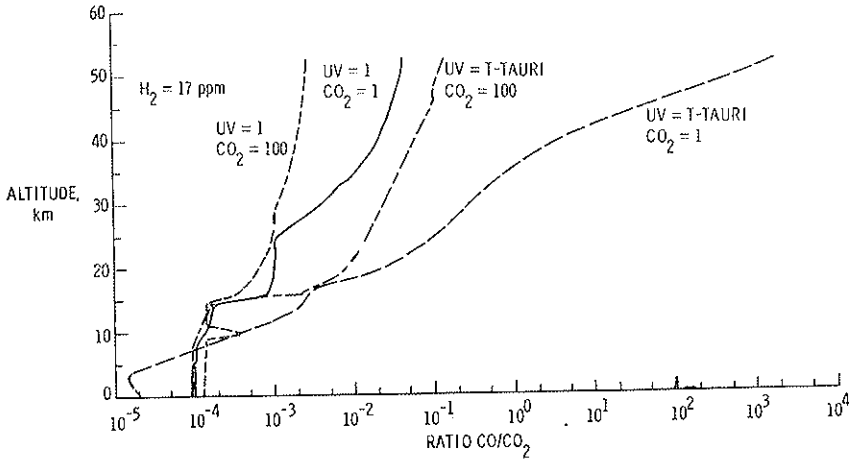

FIG. 18. Vertical distribution of the ratio of CO/CO_2 in prebiological paleoatmosphere. Calculations for molecular hydrogen (H_2) = 17 ppmv and for four different combinations of carbon dioxide (CO_2 = 1 and 100) and solar ultraviolet radiation (UV = 1 and T-Tauri).

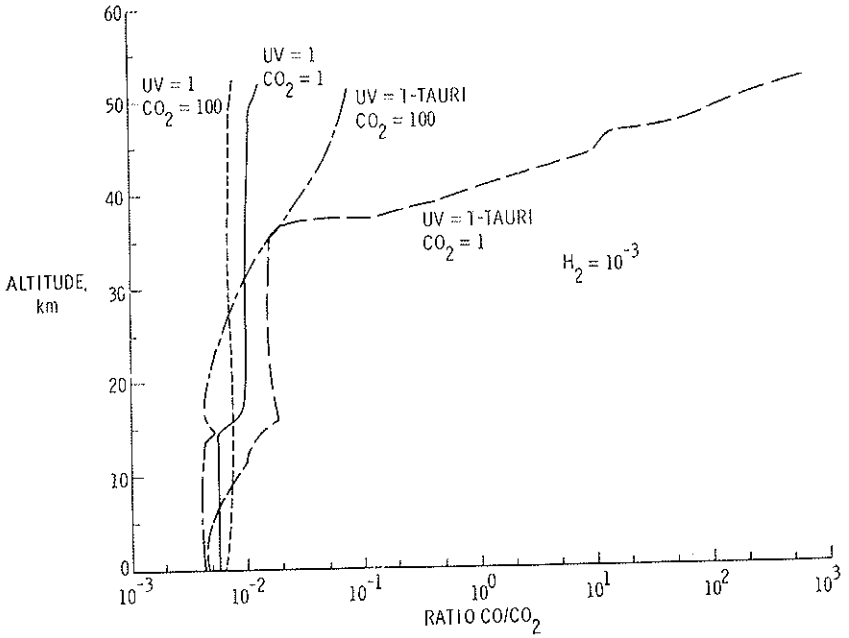

FIG. 19. Vertical distribution of the ratio of CO/CO_2 in prebiological paleoatmosphere. Calculations for molecular hydrogen (H_2) = 10^{-3} and for four different combinations of carbon dioxide (CO_2 = 1 and 100) and solar ultraviolet radiation (UV = 1 and T-Tauri).

are required for the abiotic production of organic molecules in mildly reducing atmospheric mixtures of N_2, H_2O, CO_2, and CO according to recent laboratory experiments of Bar-Nun and Chang (1983).

ACKNOWLEDGEMENT

C.L.I. thanks the IUE Observatory for its support through contract NASA 5-25774. The IUE data analysis was performed at the Regional Data Analysis Facility at Goddard Space Flight Center.

REFERENCES

ACKERMANN M., in: *Mesospheric Models and Related Experiments*, (ed. G. Fiocco), D. Reidel, Dordrecht, Holland, 149 (1971).

AGEKYAN T.A. and ANOSOVA Zh.P., « Astr. Zh. », *11*, 1006 (1968).

APPENZELLER I., CHAVARRIA C., KRAUTTER J., MUNDT R. and WOLF B., « Astron. Astrophys. », *90*, 184 (1980).

BAR-NUN A. and CHANG S., « J. Geophys. Res. », *88*, 6662 (1983).

BATCHELOR G.K., *The Theory of Homogeneous Turbulence*. Cambridge Univ. Press. (1970).

BENLOW A. and MEADOWS A.J., « Astrophysics and Space Science », *46*, 293 (1977).

BODENHEIMER P., in: *Fundamental Problems in the Theory of Stellar Evolution*, IAU Symp., (eds. D. Sugimoto et al.), Reidel Publ. Co., Dordrecht (1981).

BODENHEIMER P., « Ap. J. », *224*, 488 (1978).

BOESGAARD A.M. and SIMON T., in: *Second Cambridge Workshop on Cool Stars, Stellar Systems, and the Sun*, (eds. M.S. Giampapa and L. Golub), SAO Special Report No. 392, Volume II, p. 161 (1982).

BOSS A.P., « Icarus », *51*, 623 (1982).

BOSS A.P., « Icarus », *55*, 181 (1983).

BROWN A., JORDAN C., MILLAR T.J., GONDHALEKAR P. and WILSON R., « Nature », *290*, 34 (1981).

CABOT W., CANUTO V.M., HUBICKYJ O. and POLLACK J., *The primitive solar nobula* (Preprint, 1985).

CAMERON A.G.W., in: *The Origin of the Solar System*, (ed. S.F. Dermott), J. Wiley, N.Y., 49 (1976).

CAMERON A.G.W., « The Moon and the Planets », *18*, 5 (1978).

CANUTO V.M., LEVINE J.S., AUGUSTSSON T.R., IMHOFF C.L., « Nature », *296*, 816 (1982).

CANUTO V.M. LEVINE J.S., AUGUSTSSON T.R., IMHOFF C.L. and GIAMPAPA M.S., « Nature », *305*, 281 (1983).

CANUTO V.M., GOLDMAN I. and HUBICKYJ O., « Ap. J. Letters », *280*, 55 (1984).

CANUTO V. M. and GOLDMAN I., « Phys. Rev. Lett. », *54*, 430 (1985).

CHANDRASEKHAR S., *Hydrodynamic and Hydromagnetic Stability*. Oxford University Press (1961).

COHEN M. and KUHI L.V., « Ap. J. Suppl. », *41*, 743 (1979).

DE CAMPLI W.M. and CAMERON A.G.W., « Icarus », *38*, 367 (1979).

ELMEGREEN B.G., « The Moon and the Planets », *19*, 261 (1978); « Astr. and Astrophys », *80*, 77 (1979); *92*, 267 (1978); *64*, 173 (1978).

FALK S.W. and SCHRAMM D.N., « Sky and Telescope », *58*, 18 (1979).

FEIGELSON E.D. and KRISS G.A., « Ap. J. Letters », *248*, L35 (1981).

GAHM G.F., FREDGA K., LISEAU R. and DRAVINS D.,, « Astron. Astrophys. », *73*, L4 (1979).

GIAMPAPA M.S., CALVET N., IMHOFF C.L. and KUHI *L.V.*, « Ap. J. », *251*, 113 (1981).

GOLDREICH P. and LYNDEN-BELL D., « M.N.R.A.S. », *130*, 97 (1965).

GOLDREICH P. and WARD W.R., « Ap. J. », *183*, 1051 (1973).

GOUGH D., in: *Problems in Stellar Convection*, (eds. E.A. Spiegel and J.P. Zahn), Springer-Verlag, N.Y., 15 (1976).

GOUGH D., in: *Proceed. Workshop on Solar Rotation*, (eds. G. Belvedere and L. Paternò), Oss. Astr., Catania, Publ. No. 162, 337 (1978).

HAYASHI C., in: *Fundamental Problems in the Theory of Stellar Evolution*, IAU Sym. 93, (eds. D. Sugimoto et al.), D. Reidel Publ. Co., Dordrecht (1981).

HAYASHI C., « Prog. Theor. Phys. Supp. (Japan), in press. (1982).

HAYASHI C., NAKAZAWA K. and ADACHI I., « Publ. Astron. Soc. Japan », *29*, 163 (1977).

HERBIG G.H., « Advances Astron. Astrophys. », *1*, 47 (1962).

HERBIG G.H., in: *Spectroscopic Astrophysics*, (ed. G.H. Herbig), U. Calif. Press, Berkeley, p. 237 (1970).

HERBIG G.H., « Ap. J. », *182*, 129 (1973).

HOYLE F., « Q. J. Roy. A. Soc. », *1*, 28 (1960).

HOYLE F., in: *Origin of the Solar System*, (eds. R. Jastrow and A.G.W. Cameron), Acad. Press, N.Y. (1962).

IMHOFF C.L. and GIAMPAPA M.S., « Ap. J. », *239*, L115 (1980).

JAKOSKY B.M. and AHRENS T.J., « Proc. Lunar and Planet. Sci. Conf. 10th », 2727 (1979).

JONES B.F. and HERBIG G.H., « Astron. J. », *84*, 1872 (1979).

KASTING J.F. and WALKER J.C.G., « J. Geophys. Res. », *86*, 1147 (1981).

KUHI L.V., « Astron. Astrophys. », Suppl., *15*, 47 (1974).

LANDAU L.D. and LIFSHITZ E.M., « Fluid Mechanics », Perg. Press, London (1959).

LEDOUX P., SCHWARZSCHILD M. and SPIEGEL E.A., « Ap. J. », *133*, 184 (1961).

LEE T., PAPANASTASSIOU D.A. and WASSERBURG G.I., « Geophys. Res. Letters », *3*, 109 (1976).

LEVINE J.S. and BOUGHNER R.E., « Icarus », *39*, 310 (1979).

LEVINE J.S., AUGUSTSSON T.R., BOUGHNER R.E., NATARAJAN M. and SACKS L.J., in: *Comets and the Origin of Life*, (ed. C. Ponnamperuma), D. Reidel, Dordrecht, Holland, 161 (1981).

LEVINE J.S., AUGUSTSSON T.R. and NATARAJAN M., « Origins of Life », *12*, 245 (1982).

LEVINE J.S. and ALLARIO F., « Environ. Monitor. and Assess. », *1*, 263 (1982).

LEVINE J.S., « J. Molec. Evol. », *18*, 161 (1982).

LEWIS J.S., « Icarus », *16*, 241 (1972); « Science », *186*, 440 (1974).

LIN D.N.C. and PAPALOIZOU J., « M.N.R.A.S. », *191*, 37 (1980).

LIN D.N.C., « Ap. J. », *246*, 972 (1981).

LIN D.N.C., « Lick Observatory Contribution », N. 426 (1981).

LIN D.N.C. and BODENHEIMER P., « Ap. J. », *262*, 768 (1982).

LOW C. and LYNDEN-BELL D., « M.N.R.A.S. », *176*, 367 (1976).

MESTEL L., in: *Stellar Structure*, Univ. Chicago Press (eds. L.M. Aller, and D.B. McLaughlin) (1965).

MESTEL L., « M.N.R.A.S. », *138*, 359 (1968a); « M.N.R.A.S. », *77*, 186 (1968b).

MIZUNO H., NAKAZAWA K. and HAYASHI C., « Planet. Space Sci. », *30*, 765 (1982).

MUNDT R., WALTER F.M., FEIGELSON E.D., FINKENZELLER U., HERBIG G.H., and ODELL A.P., « Ap. J. », *269*, 229 (1983).

NAKAGAWA Y., NAKAZAWA K. and HAYASHI C., « Icarus », *45*, 517 (1981).

NAKANO T., FUKUSHIMA T., UNNO W. and KONDO M., « Publ. Astron. Soc. Japan », *31*, 713 (1979).

PINTO J.P., GLADSTONE G.R. and YUNG Y.L., « Science », *210*, 183 (1980).

PRINGLE J.E., « Ann. Rev. of Astr. and Ap. », *13*, 137 (1981).

RUNDEL D.R., « J. Atmos. Sci. », *34*, 639 (1977).

SAFRONOV V.S., *Evolution of the protoplanetary cloud and formation of the Earth and Planets*. NASA TTF-677 (1972).

SPIEGEL E.A., « Ap. J. », *138*, 216 (1963).

STAHLER S.W., SHU F.H. and TAAM R.E., « Ap. J. », *241*, 637 (1980).

STEVENSON D.J., in: *Origin and Evolution of the Earth's Earliest Biosphere: An Interdisciplinary Study*, (ed. J.W. Schopf), Princeton Univ. Press, 1983, to be published.

STEVENSON D.J., « Science », *214*, 611 (1981).

STEWART R.W. and TOWNSEND A.A., « Phil. Trans. Roy. Astr. Soc. », *243*, 48 (1951).

THOMSEN L., « J. Geophys. Res. », *85*, 4374 (1980).

TOOMRE J., « Ap. J. », *139*, 1217 (1964).

WALTER F.M. and KUHI L.V., « Ap. J. », *250*, 254 (1981).

WASSERBURG G.J., PAPANASTASSIOU D.A. and LEE T., in: *Les éléments et leurs Isotopes dans l'Univers*, (XXII Colloque Intern. d'Astrophysique, June 1978), Liege, Univ. Press (1979).

WASSERBURG G.J. and PAPANASTASSIOU D.A., in: *Essays in Nuclear Astrophysics*, (eds. C.A. Barnes et al.), Cambridge Univ. Press, 77 (1982).

WEIDENSHILLING S.J., « Icarus », *44*, 172 (1980); ibidem, *22*, 426 (1974); ibidem, *27*, 161 (1976).

WETHERILL G.W., « Proc Lunar Sci. Conf. 7th », 3245 (1976).

WETHERILL G.W., « Ann. Rev. Astr. Astrophy. », *18*, 77 (1980).

DISCUSSION

REVELLE

How you consider in your model the CO_2?

It is a problem for those who suggest that much CO_2 was present. In other words, they must solve this problem if they want to solve the dim sun paradox entirely. They put up so much CO_2 that they must also propose a way to remove it — which is what you are saying. They need not only an ocean, but also an efficient mechanism for removal of the CO_2. That is why I do not know whether that is the solution or not. We are using an abundance of CO_2 as usually discussed in the literature.

FIOCCO

I think I gathered from one of the slides that you kept the temperature equal to the standard atmosphere.

CANUTO

I discussed this problem with my colleagues at Langley, i.e., how to hook up this computation to a radiative transfer. Yes, this is one of the things we thought we should do. For the time being, we wanted to see the changes brought about by changes in one parameter, the UV flux. In the beginning we simply boosted up the UV flux independently of the wave-length dependent, up to 300 times more. Then we did a more refined computation with a wave-length UV flux. This is very important because the absorption cross sections are very wave-lenght dependent.

CHAMEIDES

The idea is that you are looking at variations CO_2 not over a thousand years time scale but over millions of years, and the amount of CO_2 present in the oceans and the atmosphere together is controlled by the larger cycle of continental uplift and weathering of rocks and so on and so forth; and the idea is that there is some sort of feedback between temperature and the rate at which the CO_2 is put into the atmosphere and oceans together.

In fact, according to the models you can enhance the CO_2 by factors of 100 or 1000 over long geological time scales, not over a thousand years.

CANUTO

Yes, but I don't think that was the gist of his question. Actually if I understood right, I think that one must have oceans in order to start the process that you are discussing. So that his question is: how soon do you have the oceans?

REVELLE

I don't believe that you can in fact have a high CO_2 content in the atmosphere, probably only in the ocean.

CHAMEIDES

I agree that the total amount of carbon dioxide in the ocean and in the atmosphere together is controlled by a larger cycle which goes over millions of years, and the concept is that that can be upped several orders of magnitude. Apparently you could put together a consistent geochemical model for this system and argue in fact consistently, but you can argue that the model might be wrong; apparently you could consistently put together a scheme for increasing CO_2 in the atmosphere-ocean system over millions of years and a geologic time scale of factors of 100 to 1000.

ROWLAND

I am sure that the modelers who are doing a one-dimensional model in which the rate of transport is the rate of transport that is calculated to fit species in the current atmosphere, when they start applying this to a remote atmosphere, a very different circumstance, it is not at all clear that the transport rate ought to be even similar to the one that one has now. What I wonder if you have done is to take the composition of the existing atmosphere rather than a hypothetical pre-biotic atmosphere, and put in 300 times or 10^4 times ultraviolet, see what it does to the existing atmosphere and whether the then radiation transfer characteristics of that atmosphere would be appreciably different from the present atmosphere. Then you already have the parameter; you are changing the atmosphere but you are assuming that the transport characteristics are exactly the same as this atmosphere.

CANUTO

There are several comments on that. First of all, there is a path that somehow you have to follow in order to compare your results with existing ones. We only meant to change one parameter, the one that astrophysics was telling us we should change. As for your second remark: a hypothetical atmosphere, well, it is hypothetical to a certain extent. There are in fact new data available for Jupiter and Titan. The composition used may be regarded as having been suggested by Titan.

As for your last point of taking today's atmosphere and today's composition and trying just to test those kinds of things, I had not thought of it, but it is certainly feasible, and could be done. I do not know if my collaborators want to spend extra money to do it, but it is a worthwhile kind of computation. There are other problems too. For instance, the UV absorption cross-section for OH. We used a 1949 reference, like everybody else. Recently I realized that the cross-section for OH has been reworked by people at Harvard. Their results are substantially different from the ones that were available in the literature. So we have a lot of cleaning up to do, even at the level of basic things like cross sections. What we have done is a test of how sensitive is this photochemical set of reactions to an increase of one of the external parameters, the UV flux. If you judge that the response is sufficiently interesting, then you have to do all these other things.

CRUTZEN

The nitrogen chemistry would be very interesting. Did you just not yet have the time to consider that, or did you leave it out because it is unimportant?

CANUTO

I am glad you asked that question. We have published two papers on this subject. In the results I have shown today, the nitrogen chemistry was not present. However, in our previous calculations we had included it and the results are available.

ROWLAND

I think I would dispute only a little bit with you. It seems to me that when you say that everyone, everyone else that has a one-dimensional photochemical model has done this; but some of the inferences about the early

atmosphere are not dependent upon photochemical models, so that if one looks at the geological record as to when we switch from reducing to an oxidizing atmosphere or something of this sort, the kind of question that I would phrase from this is: is there anything detectable at the surface of the earth that would reflect such a change in ultraviolet flux; that is, trying to eliminate the photochemical model.

CANUTO

I wish I could give a full answer. That is the same question I asked myself several times: what does all this mean? Is there any way to check the consequences? If one takes the point of view that one believes in the new UV data — and I think we have to — then the question is: have we chosen the right photochemical reactions in order to trace the consequences? And that is why we included formaldehyde, a useful, perhaps indispensable molecule for future polymerization processes. An increased UV increases the yield of such molecule, which is a good sign. Moreover, laboratory simulation experiments tell you that you need a ratio of CO to CO_2 which the standard model does not provide. The present model does. So I would say that higher UV helps at least in two cases. Clearly this is a compatibility argument, not a proof.